



University
of Stavanger

FACULTY OF SCIENCE AND TECHNOLOGY

MASTER THESIS

Curriculum: Petroleum Engineering /
Natural Gas Technology

Spring semester, 2019

Confidential

Author: Danny Cañas

Danny Cañas

.....
(author signature)

Tutor: Runar Bøe

External Supervisor: Nikolaos Vrachatis (HeLeNGi Engineering Ltd)

Master thesis title: **LNG marine system design, critical appraisal of IGF Code requirements, parametric optimizing of design inputs and mathematical modeling of LNG/NG leakage spread in the Tank Connection Space.**

Keywords: LNG leakage spread
LNG marine system
LNG-fuelled ships
IGF code
LNG Tank Connection Space
LNG pipe leakage

Number of pages: 48
.....
+ appendices/other: 1
.....

Stavanger, 15.06.2019
.....
date/year

Acknowledgements

Firstly, I want to thank God and my family for all encouragement to me to keep working on my studies, they are witnesses of the great effort I put for achieving the goal of having high-quality education abroad.

Secondly, I also want to thank the University of Stavanger (UiS) for having chosen me to study my master in this beautiful and happiest country in the world, I just hope to have filled its expectation as student. Similarly, thanks to the HeLenGi Company in Greece for the great opportunity of letting me write the thesis for them. It is been highly valuable knowledge that I gained in the field of LNG as marine fuel, which was one of the ultimate goals of pursuing a master degree in natural gas specialization.

Finally, thank you all people and friends who helped me and supported me in some way to make me get some progress for the culmination of my studies such as my mom, dad, my brothers and sister, my family in Miami and Manizales and my Colombian friends Maria Mercedes Caceres and Alfonso Herrera who always had a word for motivation.

Summary

The European government is concerned about reducing greenhouse gas emissions due to climate change and global warming. Therefore, all sectors within the European Union are committed to achieving the Paris agreement goals, and the maritime industry is no exception. Currently, the most usable fuel as propulsion system for ships is marine gas oil, which is highly pollutant compared to natural gas. Thus, the environmental benefits obtained by shifting the propulsion system from heavy fuel to LNG are highly relevant for achieving those goals.

The case study is a retrofitted vessel (RoPax 135m) to LNG as marine fuel system with a LNG tank capacity of 500 m³. The design consists of an LNG tank and an attached tank connection space (TCS) that were made by the HeLeNGi Engineering Ltd, based on the International Code of Safety for Ships using gases or other Low-flashpoint fuels (IGF code) and International Maritime Organization (IMO) standards. The objective of this thesis, working in collaboration with HeLeNGi, was to study the possible increase in the pressure inside the TCS due to a 4" full bore LNG pipe leakage with a flow of 100 m³/h and 12 Bar pressure, during 5, 15 and 25 seconds.

For doing this, free student computational fluid dynamics (CFD) ANSYS software was used, as it has the most approachable transport phenomena equations that describe this type of problem. The first task was to understand the basics, the governing equations such as momentum, mass and energy and how to manage the software, as the starting point was from scratch. Secondly, after defining the mathematical model (multiphase Mixture model, energy equation and the turbulent viscosity equation k-epsilon) the simulation Build-up was made. This set-up consisted of developing the study geometry, that was made using the free online SOLIDWORKS software. Furthermore, the configuration of the mesh, for finding the right discretization of the system in which the iteration of the program takes place. Next, the characterization of the main parameter as well as the definition of the boundary condition inside the software. Finally, customization and determination of a suitable method and controls for monitoring the solution.

The final part of the thesis consisted of simulating a leakage during 5, 15 and 25 seconds. The obtained results indicate that under the suggested ventilation conditions by IGF code, the maximum increase in the pressure reaches 0.3 mbar. Similarly, when the LNG leakage enters the TCS, it experiences flash vaporization, reducing the concentration of the LNG to zero when the fluid flow 1 m downwards (in direction of the bottom). The temperature of the TCS remains constant (288 K) except to the vicinity of the LNG leakage hole that might get down to 111 K.

Table of Contents

ACKNOWLEDGEMENTS	ii
SUMMARY	iii
TABLE OF FIGURES	vi
LIST OF TABLES	viii
TABLE OF APPENDICES.....	ix
1 INTRODUCTION	10
2 LNG MARINE SYSTEM FUNDAMENTALS	12
2.1 Description of LNG marine components	13
2.1.1 <i>Bunkering station</i>	13
2.1.2 <i>LNG storage tank</i>	14
2.1.3 <i>LNG vaporizer and gas heater</i>	15
2.1.4 <i>Pressure built-up (PBU)</i>	15
2.1.5 <i>Gas Valve Unit (GVU)</i>	15
2.1.6 <i>Ventilation system</i>	15
2.1.7 <i>Valves and pipes</i>	15
2.1.8 <i>LNG marine system process description</i>	16
3 REAL CASE DESCRIPTION	17
3.1 LNG leakage description.....	17
3.2 Description of the case	17
3.2.1 <i>LNG tank</i>	18
3.2.2 <i>Tank Connection Space (TCS)</i>	19
4 MATHEMATICAL MODELING OF LNG/NG IN ANSYS	20
4.1 Description of ANSYS program	20
4.2 Governing equations and mathematical representation	21
5 ANSYS SIMULATION BUILT UP	25
5.1 Geometry construction	26
5.2 Construction of the mesh.....	27
5.3 Characterization and set-up of the main parameters	28
5.3.1 <i>Model</i>	29
5.3.2 <i>Materials</i>	29

5.3.3 <i>Cell Zone Conditions and Boundary Conditions</i>	30
5.4 Solution monitoring.....	31
5.4.1 <i>Methods and Controls</i>	31
5.4.1 <i>Initialization</i>	32
5.4.3 <i>Run calculation</i>	32
5.5 Customization of results.....	33
6 ANALYSIS AND RESULTS.....	35
6.1 Discretization of the geometry	35
6.2 LNG vaporization configuration within ANSYS.....	36
6.3 Post-processing of variables.....	37
6.3.1 <i>LNG volume fraction</i>	37
6.3.2 <i>Fluids flow velocity</i>	38
6.3.3 <i>Gradient pressure results</i>	41
6.3.4 <i>Temperature results</i>	41
7 RECOMMENDATIONS	43
8 CONCLUSIONS	44
REFERENCES	45
APPENDIX 1. ANSYS REPORT	48

TABLE OF FIGURES

<i>Figure 1 - Basis of the three (a, b and c) LNG system design.....</i>	<i>12</i>
<i>Figure 2 - BLNG fuelled ship bunkering stations</i>	<i>14</i>
<i>Figure 3 - LNG fuel tank.....</i>	<i>14</i>
<i>Figure 4 - LNG marine double-pipe system.....</i>	<i>16</i>
<i>Figure 5 - LNG tank</i>	<i>18</i>
<i>Figure 6 - Tank Connection Space.....</i>	<i>19</i>
<i>Figure 7 - Analytical procedure of ANSYS</i>	<i>21</i>
<i>Figure 8 - ANSYS FLUENT workbench</i>	<i>25</i>
<i>Figure 9 - Front view of the TCS geometry.....</i>	<i>26</i>
<i>Figure 10 - Details of “Mesh” inside ANSYS FLUENT</i>	<i>27</i>
<i>Figure 11 - Skewness distribution of the cell in ANSYS FLUENT.....</i>	<i>28</i>
<i>Figure 12 - Main setting up domain inside ANSYS FLUENT.....</i>	<i>29</i>
<i>Figure 13 - ANSYS FLUENT results workbench</i>	<i>33</i>
<i>Figure 14 - Convergence of the case in ANSYS FLUENT</i>	<i>34</i>
<i>Figure 15 - Improved mesh in ANSYS FLUENT.....</i>	<i>35</i>
<i>Figure 16 - Skewness and statistic of the improved mesh.....</i>	<i>35</i>
<i>Figure 17 - Mesh metric of the improved mesh.....</i>	<i>36</i>
<i>Figure 18 - LNG vaporization set up in ANSYS FLUENT.....</i>	<i>36</i>
<i>Figure 19 - FLNG volume fraction insede TC</i>	<i>37</i>
<i>Figure 20 - Fluids flow velocity after 5 s</i>	<i>38</i>
<i>Figure 21 - Fluids flow velocity after 15 s</i>	<i>39</i>
<i>Figure 22 - Fluids flow velocity after 20 s</i>	<i>39</i>

<i>Figure 23 - Velocity of the fluids</i>40
<i>Figure 24 - Streamlines of fluids velocity</i>	40
<i>Figure 25 - Gradient pressure contours</i>41
<i>Figure 26 - Temperature contours</i>42

LIST OF TABLES

Table 1 - Boundary condition for mas flow..... .30

Table 2 - Boundary condition for temperature..... .30

Table 3 - Boundary condition for pressure..30

Table 4 - Reference values..... .31

Table 5 - Spacial discretization parameters..... .31

Table 6 - Relaxation factors for Solution Controls..32

TABLE OF APPENDICES

<i>Appendix 1 – case report</i>	48
---------------------------------------	----

1 Introduction

The environmental concern in the world is increasing every day as a result of global warming. For this reason, the energy transition from fossil fuels was put in motion by increasing natural gas consumption in all sectors such as marine transportation. Therefore, marine ships are shifting their fuel from heavy fuel oil (HFO) to liquefied natural gas (LNG). LNG is simply natural gas (mostly CH₄) that has been cooled down to its condensation point (-162 °C) under atmospheric pressure. Under liquid conditions the LNG reduces its volume 600 times, making the transportation of the gas technically feasible. As the density of the gas increases considerably after liquefaction, at ambient pressure, it becomes attractive storage and transportation of LNG.

After the natural gas (NG) is extracted from underground reservoirs, it undergoes processing and treatment processes in which contaminants, such as CO₂, H₂S, water and mercury must be removed. Under these conditions, the gas is ready to be liquefied, and the heavy component (C₃, C₄ and C₅₊) are also removed through the liquefaction process. To achieve this, the gas circulates inside refrigeration cycles and with help of refrigerant, it reaches cryogenic temperatures until its liquefaction. The most widely used liquefaction processes are Propane pre-cooled mixed refrigerant and Optimized cascade (Mokhatab, 2014). The LNG is stored at dedicated cryogenic LNG tanks, with special insulation, to avoid heat ingress and decrease to minimum, the boil-off gas (BOG). The types of onshore storage are single, double and full containment system with an average capacity of 160000 m³. In the case of small-scale LNG storage, the most common types are pressurized, atmospheric and floating storage regasification units (FSRU) with typical capacity up to 5000 m³ (International Gas Union, 2014). For LNG marine shipping, LNG carriers can transport large capacities up to 260000 m³ and the main containment system are self-supporting prismatic type B, MOSS spherical type B and Membrane. In the case of small scale LNG shipping, some small LNG carriers have been built with a maximum capacity of 30000 m³ that are used to supply LNG to natural gas off grid areas, but most important, it is used as marine fuel or propulsion system. The most desirable and used LNG tanks in the LNG marine system are type C (also the most economical option, as it does not need a secondary barrier), designed under International Maritime Organization (IMO) standards.

This study is focusing on the use of LNG as marine fuel, the environmental benefits and the IMO 2020 fuel compliance. Some of the positive environmental benefits for the marine industry include, for example, a significant reduction in the greenhouse gas emissions of CO₂, in the exhaust combustion gases of the ship, around 25-30% compared to traditional fuels. Similarly, the reduction of NO_x by using low pressure engines (Otto cycle) and high pressure engine (Diesel cycle) is 85% and 40% respectively. In the case of SO_x and particulate matter, it can be said that emissions are almost neglectable (DNV GL, 2014).

Concerning to economic advantages, it is also found a reduction in operational and fuel costs. Through the years, since 2010, the price of LNG is been between 20% and 30% less costly than marine gasoil (MGO) (DNV GL, 2014). The company DNV GL studied one particular scenario

in the LNG AS SHIP FUEL: THE FUTURE-TODAY report 2014 in which the retrofitting of a cruise ship gives a payback time between 4-8 years, comparing prices of LNG as gas fuel with and MGO and HFO using LNG prices projections. Other important advantages include economic growth, innovation (boosting industry competitiveness) and energy securitization, as in recent years LNG is becoming more flexible and abundant (International Gas Union, 2017). A possible extension of an economic benefit for switching ship to LNG as fuel is the improvement of public health and extension of their lives as the air pollution caused by shipping contributes to respiratory diseases accelerating death, it implies an indirect negative impact on the economy.

On the other hand, some hesitations for the shifting of type of fuel have been raised as there are some technical barriers such as difficulties during retrofitting and sizing of LNG fuel tank as it takes around 1,8 times the size of Diesel oil tank or 2,5 times the size of HFO (Le Fevre, 2018). In addition to that, bunkering availability for re-fuelling ships also contributes to uncertainty as well as confusing regulatory frameworks and future LNG prices incertitude.

However, despite the fact of previously mentioned barriers and some environmental regulations placed by IMO (such as 0,5% sulphur content cap on marine fuels), the conversion from HFO and MGO to LNG, as marine fuel, has been boosted globally. According to DNV GL in the LNG is BEST FUEL of the FUTURE conference (April 2018), there are currently 247 confirmed LNG fuelled ships worldwide and 110 more LNG ready ship, as well as the projection existence of 500 LNG, fuelled ships for 2020 (Nilsen, 2018).

2 LNG MARINE SYSTEM FUNDAMENTAL

The three main types of LNG marine systems are submerged pump, pressure build-up and BOG compressor design as presented in figure 1. The submerged pump system uses a cryogenic pump located inside the LNG tank to deliver the required pressure in the engine, being the gas regasified by a vaporizer and conditioned for the gas heater to be warmed enough for combustion. The pressure build-up system consists of raising the pressure by vaporizing a small amount of LNG, when the pressure inside the tank is low, by reaching the required pressure of the engine using the build-up unit. The pressurized gas passes through the vaporizer and then the gas heater and engine. The disadvantage of this system is the fact that if there is not gas consumption by the engines, the tank pressure is easily reached its maximum working pressure, thus, it is necessary to start up the machine and consume gas to maintain normal pressure inside the tank. The BOG compressor design is used for high pressure engines in which the gas needs to be compressed at least in two compressor stages and the compressor is located after the vaporizer (Marine Service Noord, 2019).

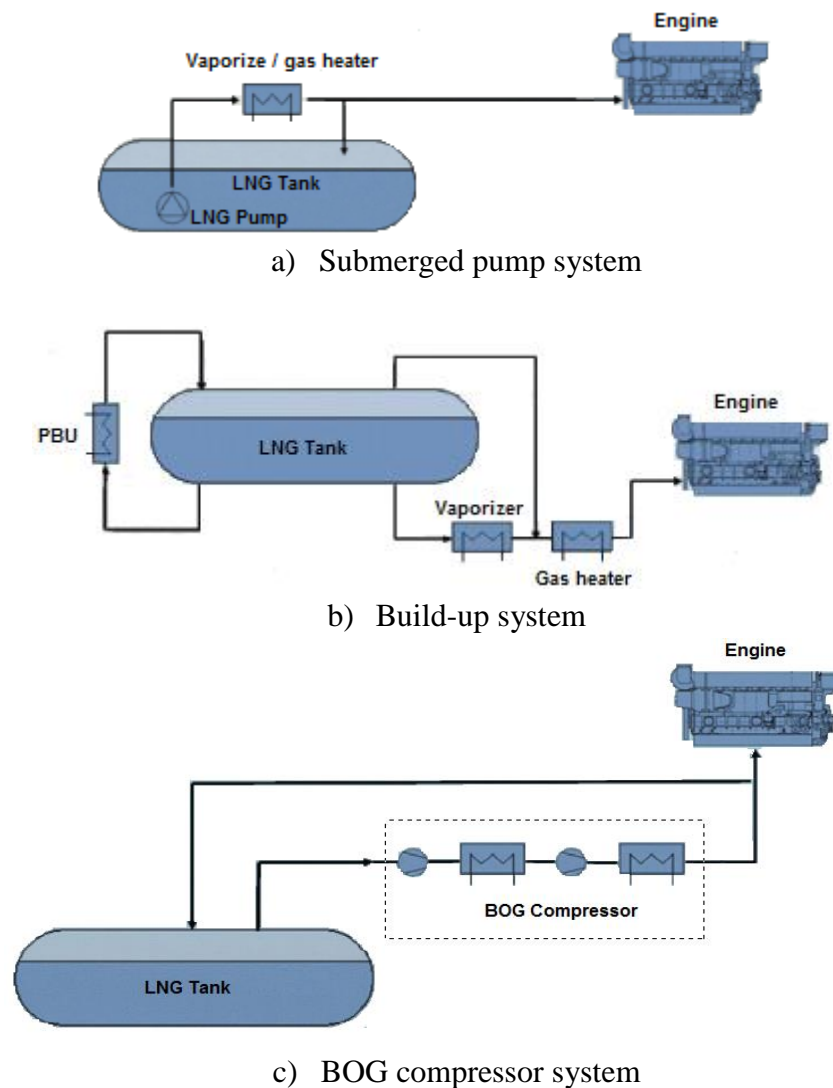


Figure 1. Basis of the three (a, b and c) LNG system design (Marine Service Noord, 2019).

In addition, the engine operation principle for gas fuelled ships is divided in two: dual-fuel (DF) engine and gas-only engine. The former can be run with diesel fuel (Diesel cycle) or gas (Otto-cycle) and operates at high pressure using a pilot fuel for starting the combustion. A certain amount of fuel (around 1% of the energy used by the engine) must be directly injected into the cylinder to be combusted with air at high temperature at the end of the compressor cycle. However, it is also possible using partly gas for running the engines up to 70% gas and the rest with diesel as well as this design is available with four-strokes and two-strokes. The latter is run just with gas and uses a spark to ignite or initiate the combustion. In contrast, compared to DF, gas-only engines operate at low pressure (5 bar) using port fuel injection.

2.1 Description of LNG marine components

The main components of the LNG fuel marine system are (Nguyen, 2015):

- Bunkering station
- LNG fuel tank
- Pressure built-up (PBU)
- LNG vaporizer
- Main gas heating system (MGH)
- Gas Valve Unit (GVU)
- Ventilation system
- Valves and pipes

2.1.1 Bunkering station

For large scale LNG bunkering process, it starts with a precooling of filling lines inside the LNG bunkering terminal by flowing LNG and returning it to the tank. After this, the connection of the bunker hose is placed and loading arms are connected between the terminal and ship by using flanges. Thus, in order to remove oxygen and moisture, inert gas (N₂) is flowed just through ship bunkering station, not for the terminal as it remains inert throughout time. In the case of small LNG bunkering, after the process of inert gas in the system, the lines are cooled down by low flow transferring LNG for the first 10 minutes. The next step is to purge the bunkering ship lines by using BOG in order to remove remaining nitrogen and then the filling sequence can start at transfer speed rate between 100 and 1000 m³/h depending on the size of the LNG tank ship. When this process is finished, the liquid line stripping is made and the process of inert the liquid lines starts by using N₂ to remove the remaining natural gas inside lines. Finally, disconnection is made by removing the hose connection between the terminal and ship. The figure 2 illustrates the bunkering system with the use of a cryogenic pump.

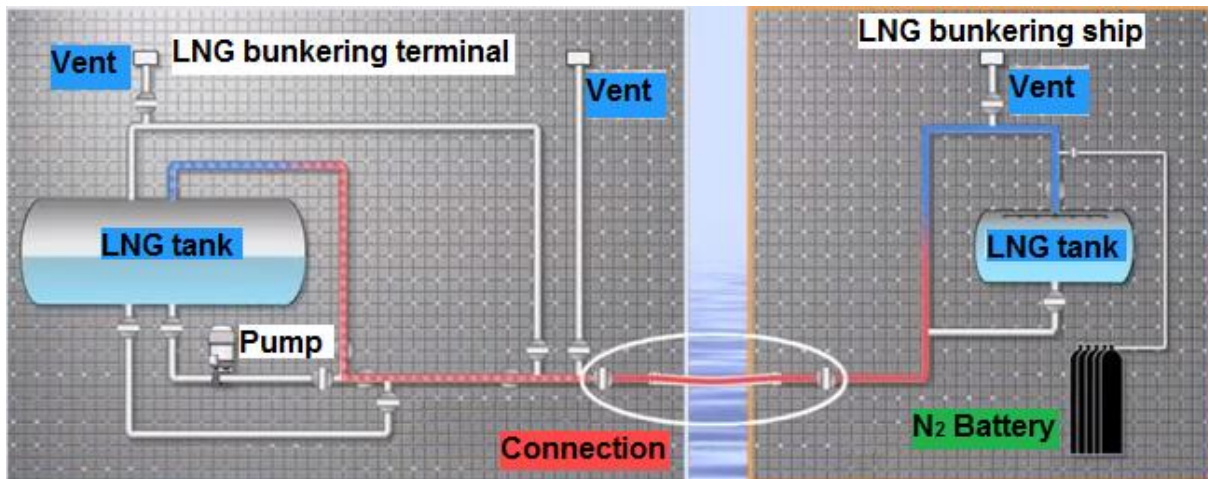


Figure 2. LNG fuelled ship bunkering stations (DNV GL, 2014).

2.1.2 LNG storage tank

The LNG fuelled ships mostly use pressurized tanks type C (working pressure between 6 - 10 bar) with spherical or cylinder shape, which can be designed according to international rules such as IMO, International Gas Carrier Code (IGC), DNV rules and other Class society Rules and Guides. These types of tanks are built with a double wall and vacuum insulation without a secondary barrier. One of the most important challenges to be addressed is the BOG rate which is a function of the LNG loading temperature and the insulation efficiency of the tank. The BOG can be vented to the atmosphere (last way of protection), flared it, used as gas fuel or re-liquefied it by returning it into the tank. According to the IMO regulation, the maximum loading limit of the LNG tank, while bunkering, is 98% of the allowable volume. In terms of usable LNG tank capacity, a common practice is to leave 5% of the volume for keeping the tank cold for next bunkering (European Union, 2015). The figure 3 illustrates an LNG fuel tank.



Figure 3. LNG fuel tank (European Union, 2015).

2.1.3 LNG vaporizer and gas heater

The vaporizer uses hot water mixed with glycol as heat source in order to vaporize the LNG into natural gas. The most popular vaporizers used within the LNG marine system is the shell and tube heat exchanger. A sub-system within the LNG vaporizer is used to move the heating source fluid consisting of two circulation pumps connected in parallel, one expansion vessel and one heat exchanger for heating the water/glycol mix. The purpose of the gas heater is to heat the vaporized gas to adequate engine temperature (China Classification Society, 2013).

2.1.4 Pressure built-up (PBU)

The pressure built-up unit is a heat exchanger that uses water-glycol brane (as in the evaporator) as the main heat source. Its main function is to control the pressure within the LNG fuel tank by maintaining it under engine pressure requirements. This is achieved by evaporating LNG (while gas consumption in the engine) and returning the vaporized gas into the LNG tank. The PBU unit also has safe control systems which include temperature sensors, vent valves and security valves.

2.1.5 Gas Valve Unit (GVU)

The GVU is located between MGH and the gas engine and its ultimate goal is to regulate feed gas pressure to the engine and to guaranty a timely and reliable shut-down of gas supply. The configuration of the GVU is a set of double block and bleed valves, 2 quick closing valves and one ventilation valve. These closing valves are designed to ensure redundancy installed in series ready to be closed in the case of loss of air supply or power. The control system of the GVU is responsible for providing a stable range of pressure to the engine. The design of GVU is based on the International Code of Safety for Ships Using Gases or other Low-Flashpoint Fuels (IGF Code) (Karlsson et al., 2013).

2.1.6 Ventilation system

The ventilation system plays a critical role in the design of a safe LNG marine system. Its main function is to avoid and remove any gas accumulation inside the Tank Connection Space (TCS). It consists of an inlet and outlet electric fans and their capacity has to be designed to provide at least 30 air changes volume per hour, based on the total volume of the room (BUREAU VERITAS, 2017).

2.1.7 Valves and pipes

The main types of valves used in the LNG marine system are control valves to regulate NG and LNG flow, emergency shut-down (ESD) and globe valves. They are constructed under IGF code for cryogenic operation, with stainless steel material, capable to work in the range of temperature between -196°C and 100°C . The most desirable valves within the LNG marine system are the globe valve because of their easy maintenance and flexibility for working under low and high pressure, compared to other valves.

The main objective of the LNG pipes is to be capable of absorbing thermal expansion or contraction caused by low temperatures of the gas without developing considerable stresses for the pipe materials. According to the IGF code the material for constructing the pipes is stainless steel and the pipes might be made with single or double-pipe system. The latter consists of an inner pipe (transportation of LNG media) and encasing pipe than can act as a secondary barrier. The insulation system for the pipes uses a thick layer of perlite, fiberglass or calcium silicate between the inner and outer pipes. To improve the insulation system, it is also possible to create a vacuum gap between the insulation layer and the encasing pipe (Nguyen, 2015). The figure 4 illustrates a double-pipe system.



Figure 4. LNG marine double-pipe system (Nguyen, 2015).

2.1.8 LNG marine system process description

For this study, the considered type of LNG marine system is pressure build-up. The process starts when the LNG is transferred from the bunkering station to the cryogenic LNG tank in the ship, in which the LNG is storage at the right pressure (in general 4-5 bar but it might be greater). Then, the PBU takes place in the process by raising the pressure at the engine required level, as the system is not equipped with a compressor or cryogenic pump. For doing this, some LNG in the tank is vaporized and re-circulated between the storage tank and the PBU until reaching the desired pressured. Furthermore, LNG is sent to the evaporator to be regasified to the engine required temperature. In this case, the evaporator acts as a vaporizer and heater as the MGH will not be used for this study. Finally, the GVU takes the gas and regulates its pressure according to engine necessities to have a smooth fuel gas supply system and reliable safe system disconnection in case of shut down. It is located inside the TCS.

3 REAL CASE DESCRIPTION

3.1 LNG leakage description

The LNG leakage phenomenon at high pressure is not been widely studied around the world, hence, the information available in the literature is limited. However, some few specific cases have been studied an LNG leakage in confined space or TCS case under low pressure conditions. For example, Li, Zhou and Konovessis, (2016) used Computational Fluid Dynamics (CFD) for simulating a LNG leakage in a pipe inside the TCS at 2 bar, concluding that the LNG leakage has the form of jet flow and the size and dispersion depend on leakage rate, position and direction of the release, temperature, ventilation and machinery located inside TCS. Similarly, Sung et al., (2016) studied the influence of crack size of an LNG leakage, using CFD tools, and the results showed in the simulation that a jet flow is formed, obtaining a risk region of a candle shape as well as the transverse and longitudinal distance of the jet increase with the crack size. In addition, Li et al., (2017) studied an LNG leakage at high pressure (40 bar) in a confined space, conducting numerical experiments, in order to develop an engineering modeling for prediction of the lower flammable limit (LFL) of an LNG jet flow leakage. Kim et al., (2011) used CFD to study overpressures due to vapor cloud explosions as well as to analyze an LNG leakage dispersión, to find the most relevant variables for risk of explosion.

Therefore, an LNG marine system under pressure conditions is expected to an LNG pipe leakage leads for a jet flow. According to Health and Safety Laboratory (2010), there could be three forms of the jet: stable liquid jet, mechanically fragmented jet and two phase jet. The stable liquid jet is caused because of a small amount of heat received by the jet and it remains liquid until hitting a surface in which a pool is created. The mechanical fragmented jet is formed by droplets, big enough to fall to the floor but once they start falling, the surface area ratio of the particles is small enough to be vaporized by the air, with the possibility of not being completely vaporized and then a small LNG pool might be formed on ground. Finally, the two-phase jet is caused because of LNG high pressure operation, in which a rapid de-pressurized due to the crack of the pipe, cause vaporization of some particles, showing 2 phases in the leakage and the resultant fluid is a fine aerosol spray cloud with some small droplets in the air.

3.2 Description of the case

For this study, high pressure LNG release is considered and the ultimate objective of this study is to estimate the maximum pressure possible at the inside of the TCS after an LNG leakage and the side effects of this. Similarly, the concentration of gas inside the TCS will be also determined. For doing this, the propulsion system of a 135 m ship RoPax will be retrofitted with an LNG tank capacity of 500 m³ and the LNG TCS equipment (size, ventilation openings, etc.) will be considered. The main scenario that is going to be simulated using student Computational Fluids Dynamic (CFD) ANSYS software version 19.2, is DN100 (4") pipe with an LNG flow of 100 m³/h and 12 bar. Under this condition, three different cases are to be considered in which 5, 15 and 25 seconds leakage will be studied.

3.2.1 LNG tank

The figure 5 illustrates the proposed LNG tank for the retrofitting of the ship. The selected kind of tank is type C with a capacity of 500 m³ and its main design parameters are based according to IGF code. This code suggests formulas and some design conditions for calculating the pressure of the vessel, shell thickness, allowable stresses, pressure-relieving system, sizing vent pipes and consideration of different types of loads such as thermal, dynamic sloshing and test loads. The tank body has a length of 18 m and a diameter of 6.2 m. The spherical part of the tank has a radius of 3.1 m.

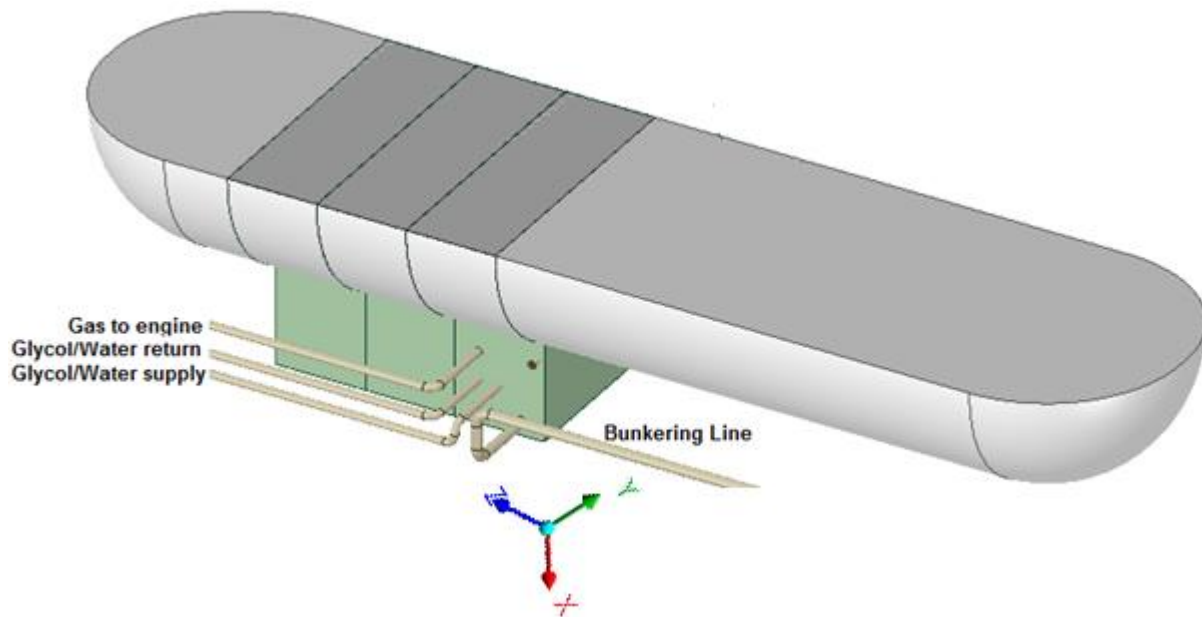


Figure 5. LNG tank (HeLeNGi, 2019).

For this case, the tank required no secondary barrier for gas fuel containment system as the probability of leakage due to structural failure is considerably low, therefore it could be neglected. In addition, in order to protect the hull of the ship for reaching low temperatures, thermal insulation is provided, as recommended by the IGF code, by avoiding any flux of heat from the tank. Finally, the selected materials for the tank is based on IGF code recommendation, corresponding to those that can able to support the lowest temperature (temperature of the fuel) during the worst-case scenario (maximum leakage).

For the purpose of simulating the case scenarios, the geometric of an LNG tank needed to be designed by using the online version program of SOLIDWORKS. This program is widely used in the engineering field for simulating geometries of any type of figures. For doing the design more practical, just half of the tank is required calculations as shown in the figure 5. This geometric must be introduced within the simulator as it is one of the input parameters that ANSYS required, in which the computational fluids dynamics models of the program will be applied. The geometric of the tank also was assembled with the TCS (green boxes) by using SOLIDWORKS as shown in figure 5.

3.2.2 Tank Connection Space (TCS)

The figure 6 shows the design of the tank connection space configuration made by HeLeNGi. This design is configured to withstand the maximum pressure build-up during any possible leakage as recommended by the IGF code. Within the figure is also possible to see directions of the fluids such as bunkering line, gas from LNG tank to engine and supply and return of the main source of heat (glycol/water brane) to vaporize the LNG in the vaporizer.

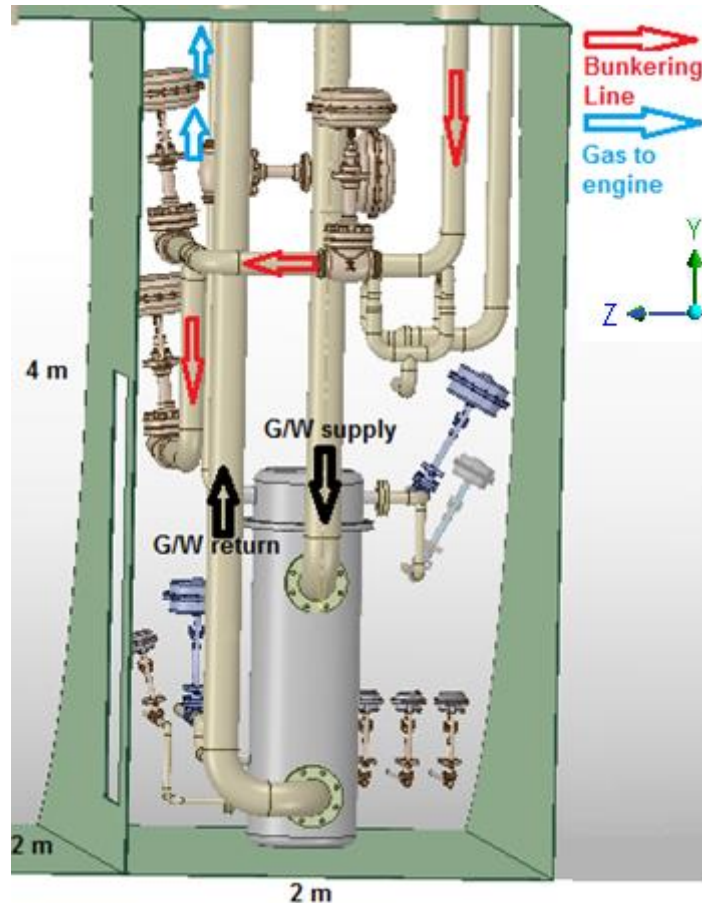


Figure 6. Tank Connection Space (HeLeNGi, 2019).

The figure 6 also describes the dimensions of the TCS 4 m x 2m x 2m with the major equipment inside such as the LNG vaporizer, manhole, control valves and the gas to engine, bunkering and glycol/water pipes. The inlet and outlet ventilation are not included in the graph; however, they are considered within the simulation in ANSYS with dimensions of the vent air inlet of DN300 (12”) and vent outlet whole of DN300 (12”). The exact location of the leakage is situated in the bunkering line at the top of the TCS where the line connects with the same top, in direction of the fluid flow from bunkering to LNG tank, with a full-bore breakage and pipe diameter (DN100 / 4”).

The detailed TCS geometry was designed on SOLIDWORK, including main components to be assembled it, with the LNG tank geometry. As mentioned above, the full obtained geometry is introduced in ANSYS as a mandatory input parameter for the simulation.

4 MATHEMATICAL MODELING OF LNG/NG IN ANSYS

For the resolution of this LNG leakage case is necessary to use computational fluid dynamics models. The ANSYS software models are based on CFD tools, capable to model compressible and incompressible fluids behavior as well as turbulent and laminar flow problems. Similarly, those models also consider transient and steady states. It is demonstrated that ANSYS is a powerful and flexible tool that provides accurate results and prediction of fluid phenomena. The most usable analysis system within the program for modeling this type of problem is CFX and FLUENT, both based on in the same governing equations but with slight differences for approaching the solution of the problem. For this thesis, the simulation is made with ANSYS FLUENT, as it has a wider range of applicability compared to CFX. Its applications include single or multiphase non-Newtonian flows with the ability to process complex geometries. FLUENT includes a package of models, volume-of-fluid (VOF), Mixture, Eulerian and discrete phase model (DPM), that can be used for modeling any possible interaction between gas-liquid-solid (ANSYS, Inc, 2013).

The mixture model, used in this simulation, is one of the most simplified multiphase models that include modeling of n phases by solving the continuity, momentum and energy equations as well as volume fraction equation for all components of the mixture. The advantage of this model is that it can perform multiphase models by solving a small number of equations compared to the Eulerian model by obtaining reliable results (ANSYS, Inc, 2013). However, all those models have some limitations within their performance, in the case of the Mixture model, conflicts are presented while modeling inviscid fluids, solidification and melting working in conjunction, among others, yet these are not the case for the simulation in this thesis.

4.1 Description of ANSYS program

The analytical procedure within any ANSYS simulation is presented in the figure 7. The black box represents the ANSYS tool in which user inputs are introduced in the program, such as the geometry of the figure that is being studied, a mesh that indicates the discretization of the geometry into cells and the boundary conditions or initial conditions of the problem. The obtained results of the simulation are given in a spectrum of colors indicating the magnitude of the studied variable. Other results are also displayed like graphs, tables and numerical results.

The user inputs are based on the physical problem that is entered in the black box, to solve a mathematical model with some embedded physical assumptions. Then, after processing and solving the variables using the finite volume method, the tool obtains numerical solutions for selected variables that were set from before to be determined, such as pressure, velocity or temperature, in a selected point of the geometry (corners, centers, mid-sides or cells). Further, those selected variables at selected points must be presented in colored pictures for getting friendly illustrative results (this process is called post-processing). Finally, hand calculations can be done based on empirical data or experimental data to have approximate estimations about

what could be the expected results, then the results might be compared. Ideally, the obtained results in ANSYS must be compared to experimental data (Courses.edx.org, 2018).

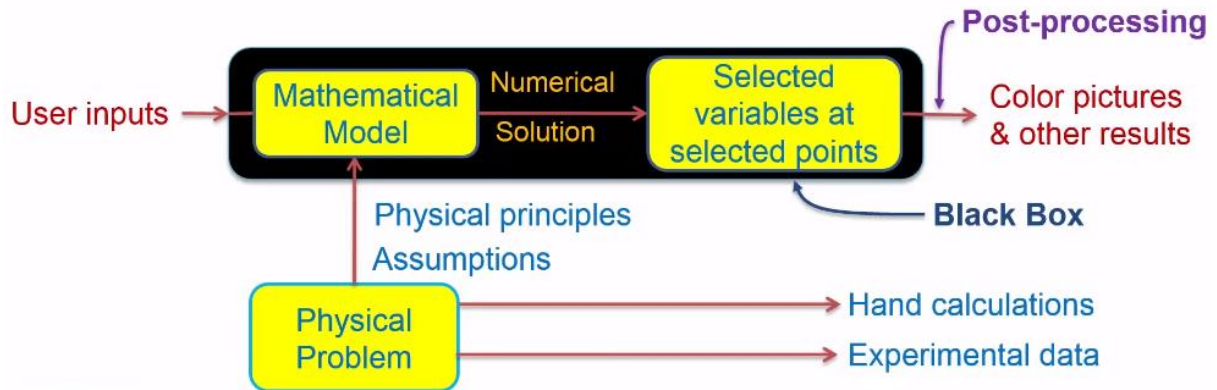


Figure 7. Analytical procedure of ANSYS (Courses.edx.org, 2018).

4.2 Governing equations and mathematical representation

To describe accurately the LNG leakage phenomenon, the conservative equations of momentum, continuity, energy, transport and viscous turbulent model are the most suitable for modeling gas behavior. The Mixture model within ANSYS is based on the next equation (Courses.edx.org, 2018):

CONTINUITY equation:

$$\frac{\partial \rho}{\partial t} + \left(u \frac{\partial \rho}{\partial x} + v \frac{\partial \rho}{\partial y} + w \frac{\partial \rho}{\partial z} \right) + \left(\rho \frac{\partial u}{\partial x} + \rho \frac{\partial v}{\partial y} + \rho \frac{\partial w}{\partial z} \right) = 0 \quad (1)$$

where ρ is the fluid density and u , v and w are the fluid velocity in x , y , z cartesian coordinates, which is valid for compressible and incompressible fluids.

MOMENTUM equations in x , y , z direction:

$$\frac{\partial (\rho \vec{V})}{\partial t} = -\nabla p - \nabla (\rho \vec{V}) \vec{V} - \nabla \tau + \rho \mathbf{f} \quad (2)$$

Where p is the static pressure, τ is the stress tensor and \mathbf{f} is the external body forces. This conservation of momentum equation is also known as the Reynolds-Average Navier-Stokes equation (Löhner, 2001) and the extent of its respective cartesian coordinates are given by the equation 3,4 and 5 as follow:

$$\frac{\partial}{\partial t} \rho u = -\frac{\partial p}{\partial x} - \left(\rho u \frac{\partial u}{\partial x} + \rho v \frac{\partial u}{\partial y} + \rho w \frac{\partial u}{\partial z} \right) - \left(\frac{\partial}{\partial x} \tau_{xx} + \frac{\partial}{\partial y} \tau_{yx} + \frac{\partial}{\partial z} \tau_{zx} \right) + \rho f_x \quad 3)$$

$$\frac{\partial}{\partial t} \rho v = -\frac{\partial p}{\partial y} - \left(\rho u \frac{\partial v}{\partial x} + \rho v \frac{\partial v}{\partial y} + \rho w \frac{\partial v}{\partial z} \right) - \left(\frac{\partial}{\partial x} \tau_{xy} + \frac{\partial}{\partial y} \tau_{yy} + \frac{\partial}{\partial z} \tau_{zy} \right) + \rho f_y \quad 4)$$

$$\frac{\partial}{\partial t} \rho w = -\frac{\partial p}{\partial z} - \left(\rho u \frac{\partial w}{\partial x} + \rho v \frac{\partial w}{\partial y} + \rho w \frac{\partial w}{\partial z} \right) - \left(\frac{\partial}{\partial x} \tau_{xz} + \frac{\partial}{\partial y} \tau_{yz} + \frac{\partial}{\partial z} \tau_{zz} \right) + \rho f_z \quad 5)$$

The stress tensor τ for each direction component is given by the equation 6, 7, 8, 9, 10 and 11, where μ is the molecular viscosity:

$$\tau_{xx} = -2\mu \frac{\partial u}{\partial x} + \frac{2}{3} \mu (\nabla \cdot \vec{V}) \quad 6)$$

$$\tau_{yy} = -2\mu \frac{\partial v}{\partial y} + \frac{2}{3} \mu (\nabla \cdot \vec{V}) \quad 7)$$

$$\tau_{zz} = -2\mu \frac{\partial w}{\partial z} + \frac{2}{3} \mu (\nabla \cdot \vec{V}) \quad 8)$$

$$\tau_{xy} = \tau_{yx} = -\mu \left(\frac{\partial u}{\partial y} + \frac{\partial v}{\partial x} \right) \quad 9)$$

$$\tau_{yz} = \tau_{zy} = -\mu \left(\frac{\partial v}{\partial z} + \frac{\partial w}{\partial y} \right) \quad 10)$$

$$\tau_{xz} = \tau_{zx} = -\mu \left(\frac{\partial w}{\partial x} + \frac{\partial u}{\partial z} \right) \quad 11)$$

ENERGY equation:

The equation 12 presents the energy model equation where C_v is the specific heat of the fluid, T is the fluid temperature and q is the heat transfer within the phases:

$$\begin{aligned} \rho c_v \left(\frac{\partial T}{\partial t} + u \frac{\partial T}{\partial x} + v \frac{\partial T}{\partial y} + w \frac{\partial T}{\partial z} \right) &= - \left(\frac{\partial q_x}{\partial x} + \frac{\partial q_y}{\partial y} + \frac{\partial q_z}{\partial z} \right) \\ - \left(\tau_{xx} \frac{\partial u}{\partial x} + \tau_{yy} \frac{\partial v}{\partial y} + \tau_{zz} \frac{\partial w}{\partial z} \right) &- T \left(\frac{\partial p}{\partial T} \right)_p \left(\frac{\partial u}{\partial x} + \frac{\partial v}{\partial y} + \frac{\partial w}{\partial z} \right) \\ - \left(\tau_{xy} \left(\frac{\partial u}{\partial y} + \frac{\partial v}{\partial x} \right) + \tau_{xz} \left(\frac{\partial u}{\partial z} + \frac{\partial w}{\partial x} \right) + \tau_{yz} \left(\frac{\partial v}{\partial z} + \frac{\partial w}{\partial y} \right) \right) & \end{aligned} \quad 12)$$

TRANSPORT equation:

The transport equation model (equation 13) is used in ANSYS Fluent for describing single-phase or multiphase flow. In this equation, C represents the mass fraction of each species and J the diffusion flux for the species (Wendt, 2009).

$$\frac{\partial}{\partial t} (\rho \mathbf{c}) + \nabla (\rho \vec{u} \mathbf{c}) = -\nabla \vec{J} \quad 13)$$

VISCOSITY TURBULENT equations:

The conservation equation for the k - ϵ turbulent flow model is presented in the equation 14, where k is the turbulent kinetic energy, u is the fluid velocity, μ_t is the turbulent viscosity, G_k indicates the generation of turbulent kinetic energy because of the mean velocity gradient, G_b represents the generation turbulent kinetic energy caused by the buoyancy, Y_M is the source term that corresponds to fluctuating in dilatation of compressible turbulence to the dissipation rate and σ_k is one of the turbulent model coefficients (Sung et al., 2016).

The equation 15 shows the conservation equation for the turbulent kinetic energy dissipation rate ϵ , where μ_k is the turbulent viscosity and C_μ is a constant of the model that has been determined experimentally by ANSYS. The purpose of the viscosity turbulent equation is to consider the effect of turbulent fluctuations of velocities within multiphase flow, however, to model this phenomenon in combination with other governing equations turns in a large number of equations, making the process extremely complex.

$$\frac{\partial}{\partial t}(\rho k) + \frac{\partial}{\partial x_i}(\rho k u_i) = \frac{\partial}{\partial x_i} \left[\left(\mu + \frac{\mu_t}{\sigma_k} \right) \frac{\partial k}{\partial x_j} \right] + G_K + G_b - \rho \epsilon + Y_M \quad 14)$$

$$\frac{\mu_t}{\rho} = \frac{C_\mu k^2}{\epsilon} \quad 15)$$

5 ANSYS SIMULATION BUILT UP

After the analysis and description of the problem and the understanding of the mathematical models that ANSYS uses for resolving the equations, the next step is to set up the simulation conditions within the program. The main platform or workbench consists of a set of computational fluid dynamics packages such as CFX and FLUENT, which the latter is chosen to be used in this work due to its suitability for modeling compressible fluid flow. After selecting the desired CFD package, the built up of the simulation is based on 5 steps: geometry construction of the solid where the phenomenon is happening, construction of the mesh in which the geometry is discretized or divided into cells, the set-up and characterization of the main parameters of the simulation (such as models, material and boundary conditions), and definition of the solution monitoring such as methods and controllers (Courses.edx.org, 2018). Finally, the customization of the obtained result for displaying the graphs, animations, plots and reports of the outcomes. The figure 8 shows the workbench of ANSYS version 19.2

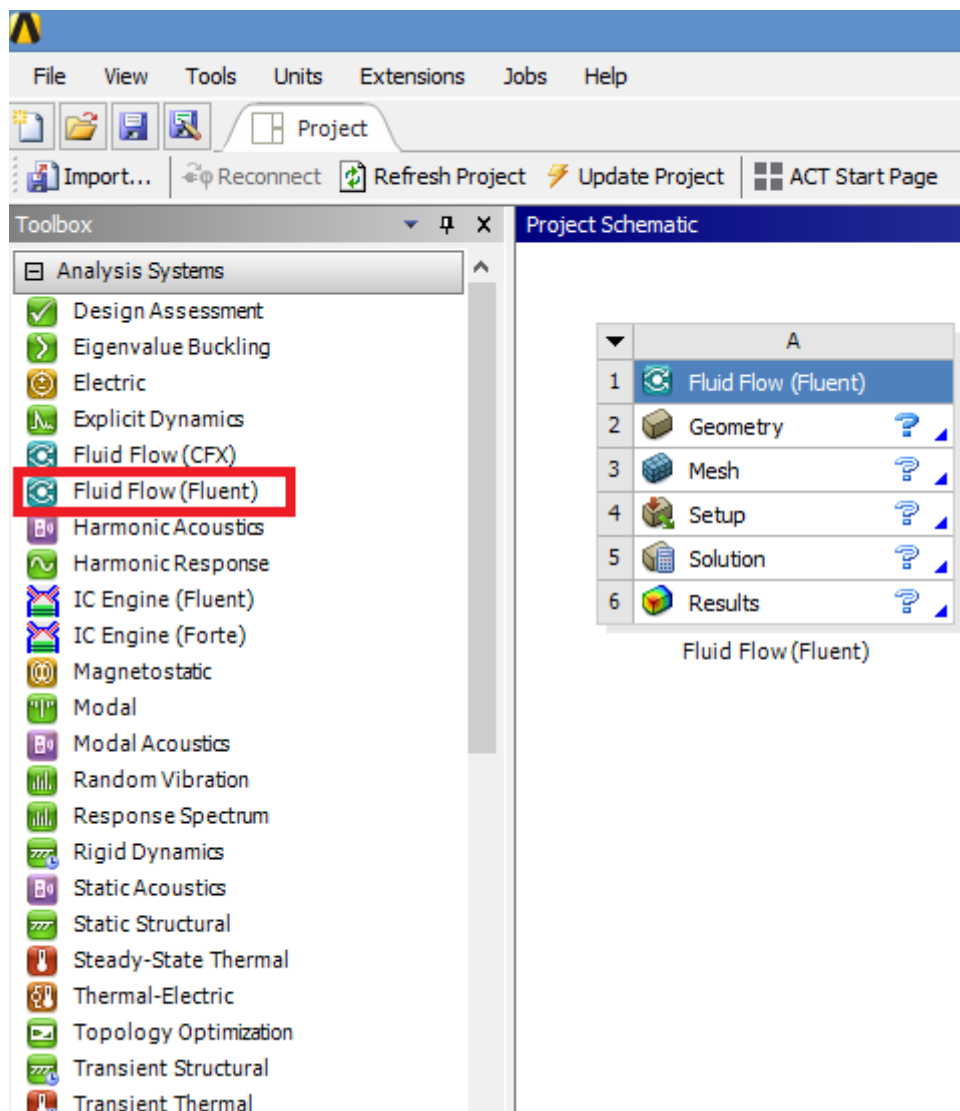


Figure 8. ANSYS FLUENT workbench.

5.1 Geometry construction

As mentioned above, the construction of the LNG tank and the TCS geometry was made using the SOLIDWORKS software (free online version). The resulted file is compatible with the design modeler bench of ANSYS, therefore, the SOLIDWORK files can be easily imported. Within the design of the TCS geometric, in order to understand the phenomena, a simplified model was developed, consisting of an empty box (without considering pipes and valves) with the same dimension as the TCS 4000 mm x 2000 mm x 2000 mm. This box presents an LNG Inlet leakage hole in the top corner of the room, Outlet vent hole on top and an Inlet vent pipe going from the top of the box to 0,5 m above the floor. The ultimate goal of this configuration is to allow air flow inside the TCS from the bottom to the top and drag the vaporized gas into the outlet vent. As indicated in the IGF code, the vent systems must have the capacity of removing 30 times the volume of the TCS per hour (BUREAU VERITAS, 2017). In this case, the volume of the TCS corresponds to 16 m³, thus, the mass flow inlet setting inside the boundary conditions is 480 m³/h (0.16 Kg/s). In reality, electric fans are installed with the capacity to provide this necessary air inlet. The figure 9 reveals the geometry and configuration of the simplified model in ANSYS with a front view.

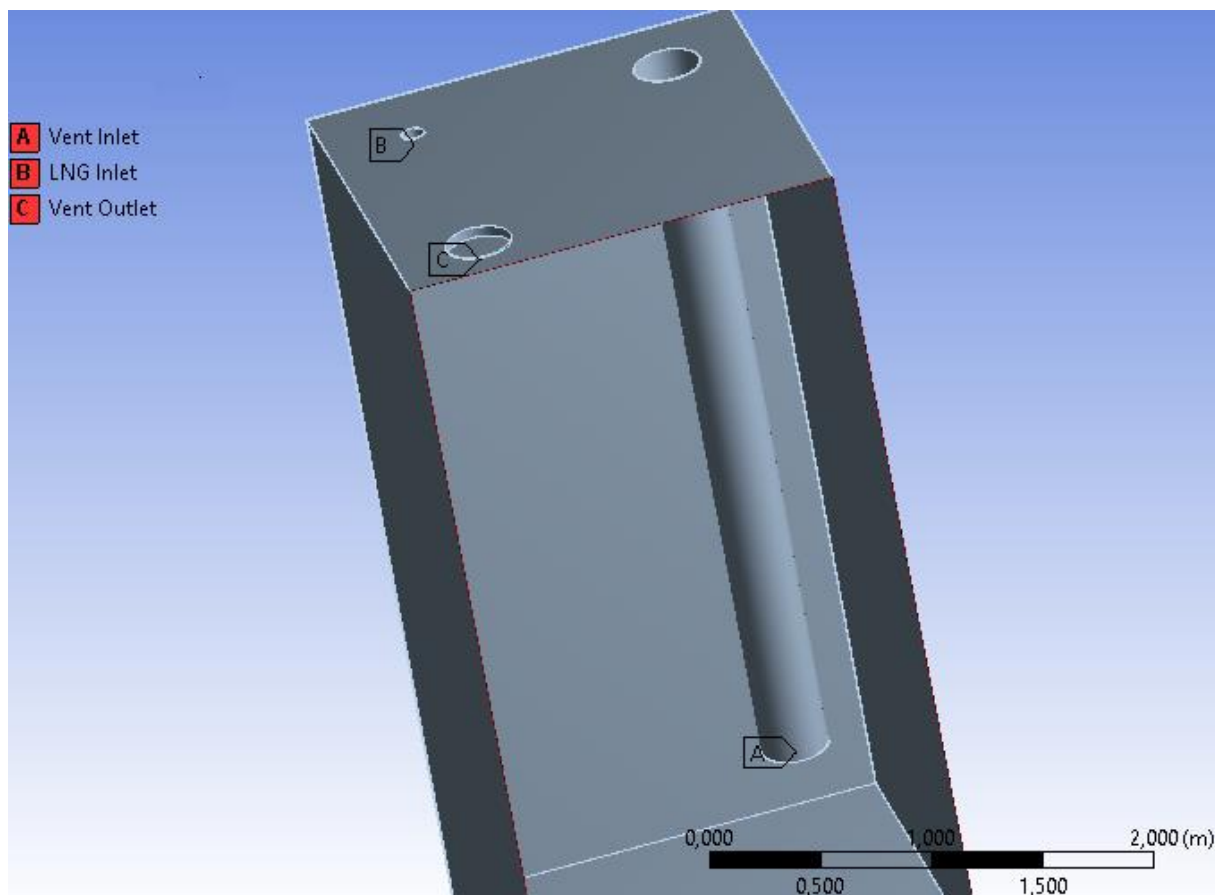


Figure 9. Front view of the TCS geometry.

The vent inlet pipe length is 3.5 m with a diameter of 300 mm and the vent outlet hole and LNG inlet leakage have a diameter of 300 mm and 100 mm respectively. The distance between the centre of the 3 holes and edges in the top face is equal to 400 mm.

5.2 Construction of the mesh

The construction of the mesh is a critical point within any simulation in ANSYS, as it determines the discretization of the system, thus, errors in the final obtained results. It is also important to highlight that fine mesh leads to more accurate results (Courses.edx.org, 2018). For completing the setting of the mesh, the first step is to configure the Details of “Mesh” parameters such as Default, Sizing, Quality, Inflation, Advanced and Statistic (figure 10).

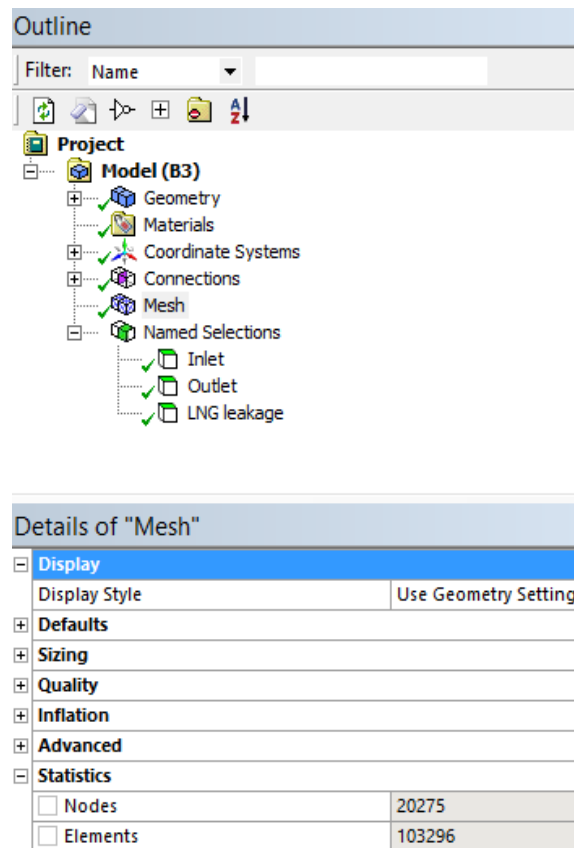


Figure 10. Details of “Mesh” inside ANSYS FLUENT.

Within the Default parameters, a linear element size of 0.24 m was selected and a growth rate of 1.2 for sizing. The former corresponds to the size of the cells and the latter is used as control sizing for its construction. The Quality parameter of the mesh is highly important for the convergence of the simulation, as the target of skewness must be defined and set lower as possible (in this case correspond to 0.9). This skewness represents how close the shape of a cell is compatible within the shape of the original geometry, affecting the stabilization of the solution in the way that high skewness numbers negatively affect the accuracy of the results (ANSYS, Inc, 2013). For example, cells with skewness between 0 and 0,25 present excellent cell quality, while cells with skewness greater than 0,9 are considered degenerate cells. The figure 11 shows the skewness distribution of the cells or elements obtained by the configuration of the mesh obtained by default in ANSYS.

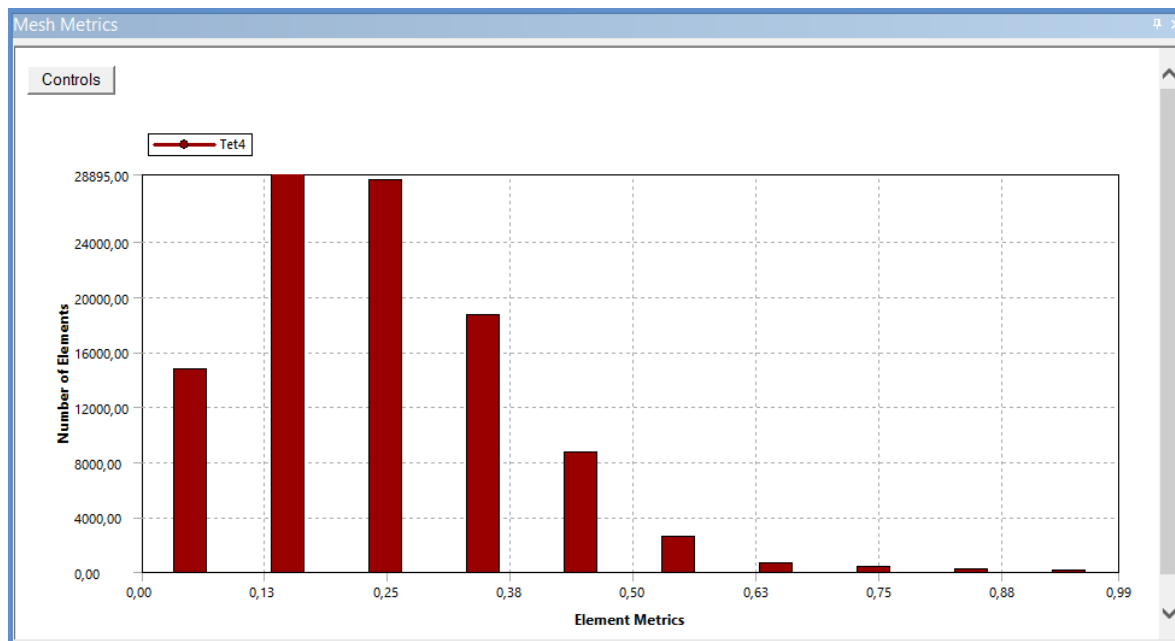


Figure 11. Skewness distribution of the cell in ANSYS FLUENT.

The Inflation and Advances parameters are set as the program recommends some standard conditions. In the case of the Statistic parameter, it is used to determine the number of cells and nodes that have been created due to the actual configuration and it is calculated by the obtained mesh. In this case, as illustrated in the figure 10, 20275 nodes and 103296 elements were obtained with current conditions. However, in order to improve the quality of the mesh, some measures can be taken such as sizing the faces of the geometry as convenient as possible and selecting a better type of mesh. In chapter 6, the obtained results of the improved mesh are presented.

After obtaining a refined mesh, the name selection or indication of the inlet and outlet areas must be created, to match them afterward with the boundary conditions. The figure 9, as presented above, reveals the Inlet, Outlet and LNG leakage areas.

5.3 Characterization and set-up of the main parameters

The figure 12 shows the displayed window of the Setting Up Domain with the main configuration parameters in the tree, highlighted in red. Within the first step of the General configuration, the type of solver must be defined, which in this case are: pressure-based, absolute velocity formulation, transient state which considers changes in the variables with time until reaching a steady state and gravity direction. Subsequently, the next tree branches to be set up are the type of Model, Materials, Cell Zone Conditions and Boundary Conditions.

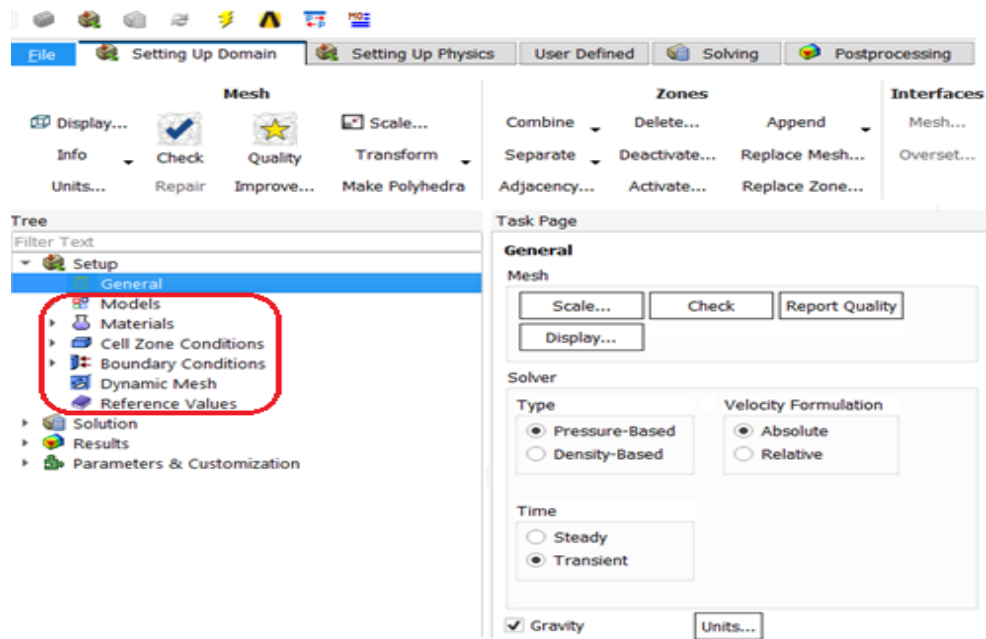


Figure 12. Main setting up domain inside ANSYS FLUENT.

5.3.1 Model

Inside the branch Model window in the tree, the Mixture model was chosen, as described above, because of its reliability by solving fluid problems for multiphase (ANSYS, Inc, 2012) compressible and turbulence flows. During the selection of this Mixture model, a sub-branch of Number of Phases involved in the process, are described and defined as primary and secondary phase (air, LNG and methane). In another sub-branch, phase interaction and interphase mass transfer must be considered from LNG phase to air phase. Therefore, the Lee model, called evaporation-condensation model and governed by the vapor transfer equation, is used in ANSYS for considering this mass transfer mechanism as well as the vaporization of the species (ANSYS, Inc, 2006). The saturation temperature of the LNG is set as 111.15 K in this configuration.

The tree branch, Energy and Viscous, are to be configured by activating Energy equations and the turbulence flow model. The latter model conditions are set as realizable k - ϵ with the near wall treatment of scalable wall function. For this turbulent model, some constant must be defined such as C2-epsilon constant, dispersion Prandtl number and energy Prandtl number (Courses.edx.org, 2018).

5.3.2 Materials

Continuing in the setting of the tree, Materials list has to be created. In this point, air and LNG are the main components that need to be defined as the entering fluids in the system. For practical purposes, LNG is mainly considered as methane, however, the main characteristics of the LNG are manually introduced in the properties window, such as density, specific heat, thermal conductivity and viscosity. Similarly, the air properties are configured according to the FLUENT database with its respective characteristics.

5.3.3 Cell Zone Conditions and Boundary Conditions

Subsequently, the branches of the tree Cell Zone Conditions and Boundary Conditions are to be set. In the former, the type of fluid that is entering the geometry must be defined (LNG and air) as well as in the latter Inlet, outlet, LNG leakage, wall solid and interior of geometry or boundary conditions, as illustrated in the table 1, 2 and 3.

Mass flow boundary conditions (Kg/s)			
	LNG	Air	Methane
Inlet	0	0.16	0
Outlet	0	0	0
LNG leakage	12	0	0
Wall solid	0	0	0
Interior	0	0	0

Table 1. Boundary condition for mas flow.

Thermal boundary conditions (K)			
	LNG	Air	Methane
Inlet	---	288	---
Outlet	0	0	0
LNG leakage	111.15	---	---
Wall solid	288		
Interior	288		

Table 2. Boundary condition for temperature.

Pressure boundary conditions (MPa)			
	LNG	Air	Methane
Inlet	0	0.1	0
Outlet	0.1		
LNG leakage	1.2	0	0
Wall solid	---	---	---
Interior	0.1		

Table 3. Boundary condition for pressure.

The last part of the boundary condition configuration is to set the reference values in the respective windows, that are used for computing normalized flow field variables (Ansyshelp.ansys.com, 2019), as shown in table 4.

Area (m ²)	1
Density (kg/m ³)	430
Entalphy (j/kg)	-4179500
Lenght (m)	1
Pressure (pascal)	0
Temperature (K)	288
Velocity (m/s)	0.0052
Viscosity (kg/m-s)	0.00015
Ratio of Specific Heats	1.4

Table 4. Reference values.

5.4 Solution monitoring

5.4.1 Methods and Controls

The setting of the Solution starts by selecting the used method for solving and defining the spatial discretization. In this case, for volume fraction, turbulent kinetic energy, transient formulation, energy and momentum, first order upwind accurate discretization scheme is selected. For the pressure spatial discretization, PRESTO scheme gives a greater approximation for the interpolation of the pressure in the face of the cells (ANSYS, Inc, 2013). First order upwind type of scheme means that the solved quantities of the variables in each cell during iteration, are calculated in the centre of the cell and represent an average value throughout the cell. Second order upwind accurate discretization achieves higher order accuracy; however, the iterative process becomes more complex (Afs.enea.it, 2019). Therefore, the first order discretization was chosen due to its simplicity, with the option of using second order after obtaining a converged solution that requires a reduction of error, then, future scalation requires more accuracy. Similarly, the pressure-velocity PISO scheme was selected as it offers a higher degree of approximation, between the correction for pressure and velocity calculations (Li, Zhou and Konovessis, 2016). The table 5 reveals the special discretization parameter of the Solution Methods.

Spacial discretization	
Pressure	PRESTO
Momentum	First order upwind
Volumen fraction	First order upwind
Turbulent kinetic energy	First order upwind
Turbulent disipation rate	First order upwind
Energy	First order upwind
Transient formulation	First order implicit

Table 5. Spacial discretization parameters.

Under the Solution Controls, relaxation factors are used for reducing fluctuations of the obtained variables, such as mass, after calculation by controlling the update of computed variables at each iteration (Ansyshelp.ansys.com, 2019). The most suitable relaxation factors are listed in the table 6. For monitoring the equation, the tools are residuals (convergence criteria) for the tolerance of mass, momentum, energy and other equations imbalance during iterations. To control until when the solver will iterate a value of 1e-06 is a suitable value (Courses.edx.org, 2018).

Under-Relaxation Factors	
Pressure	0.3
Density	1
Body force	1
Momentum	0.7
Vaporized mass	1
Slip velocity	0.1
Volumen fraction	0.5
Turbulent kinetic energy	0.8
Turbulent dissipation rate	0.8
Turbulence viscosity	1
Energy	1

Table 6. Relaxation factors for Solution Controls.

5.4.2 Initialization

The initialization process consists of assigning guess values at the cell centers as initial values such as gauge pressure or temperature. The table 7 shows the set of selected initial values for this case. It is important to mention that ANSYS suggests some values for some variables, based on previous calculations that were made with the input data given in Boundary Conditions (Courses.edx.org, 2018). The initialization method for this case is standard, which is more convenient compared to the hybrid as it allows to specify initial values manually over the whole domain.

After initializing the initial values, the next step is to patch the main variable, which in our case the LNG volume fraction must be patched zero in the walls of the geometry. However, in the LNG leakage inlet hole, this value is set as 1 as just LNG is entering into the system.

5.4.3 Run calculation

The last step in the configuration of the simulation is to run the case. Before doing that, the time step size, number of time steps and the maximum number of iterations, which in this simulation are 1 (s), 3 and 3 respectively, for a trial case. If the number of iterations and the time steps increase, the resulted solution becomes more accurate, therefore, these numbers can be modified as the user desires.

5.5 Customization of results

At this point of the simulation, the post-processing analysis inside the simulator needs to be set. Inside the simulator, a wide range of variables can be analyzed such as density, mass flow, volume fraction, pressure, temperature among others. For doing this, the most common analyses to be done are mass flow inlet and outlet balance, volume fraction in the inlet and outlet, drawing streamlines to check flow paths from inlet to outlet, introducing cross-sectional planes to identify distribution of the species inside the geometry, defining variable contour in order to see magnitude by using color spectrum, as well as tables and plots. The figure 13 shows the screenshot of the Results workbench, revealing the streamlines of the velocity of air inside the TCS. In this picture is also possible to see, on the left side in the tree, introduction of contours, planes and streamlines.

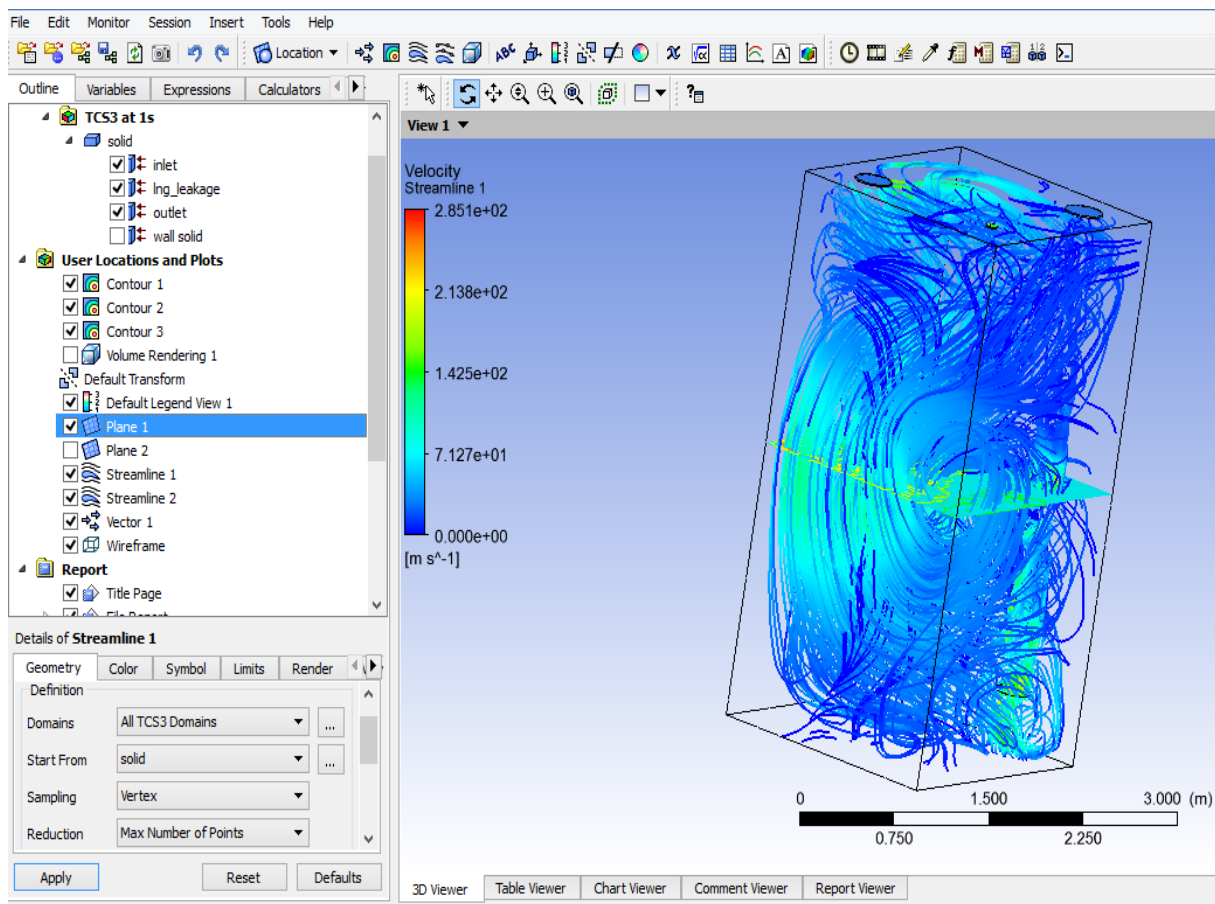


Figure 13. ANSYS FLUENT results workbench.

After completing the 5 configuration steps in ANSYS for any simulation, if the simulator finds clashes or errors in the calculation of the variables within the iterations, the computer process is interrupted. However, when the simulation converges green tick signs appear in the main ANSYS workbench. The figure 14 illustrates the convergence of a case.

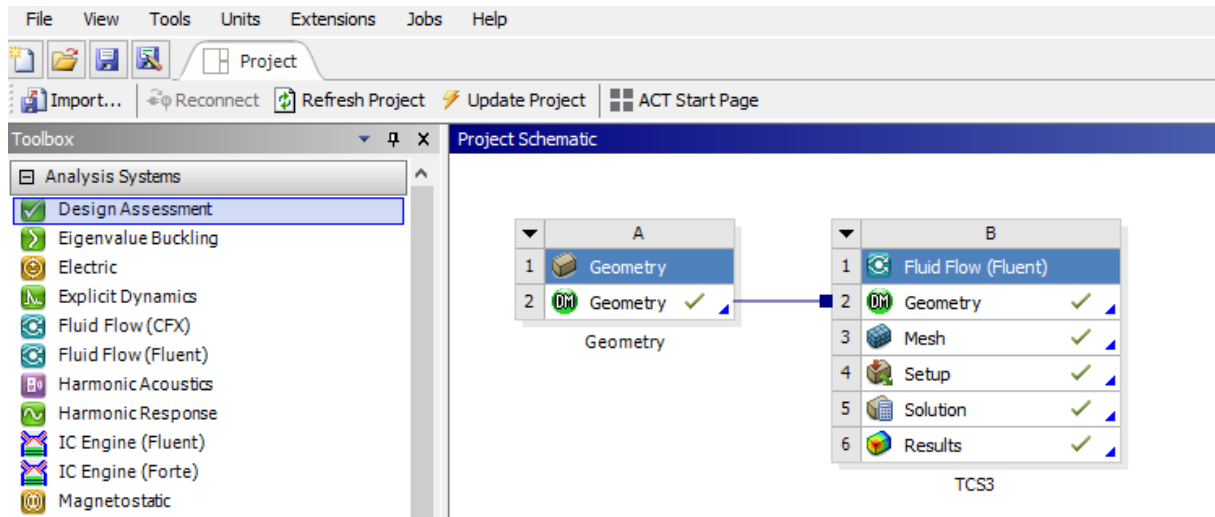


Figure 14. Convergence of the case in ANSYS FLUENT.

6 ANALYSIS AND RESULTS

6.1 Discretization of the geometry

After the construction of the geometry by using SOLIDWORKS (because of its flexibility), as illustrated in figure 9, it was introduced in ANSYS in order to set the discretization parameters. The tetrahedrons Patch Conforming Method was introduced, which is one of the most suitable types of cells to be used for the mesh control in regular geometries. Similarly, the 5 walls of the TCS, the top face and the inside pipe were sized with elements length of 0.11 m, 0.1 m, and 0.02 m respectively. As it is well known, the results accuracy increase with smaller element size, reason why the smallest size cells were implemented in the pipe, which in this case is the most critical part due to its complexity compared to other faces. The improved mesh of the discretization is presented in the figure 15.

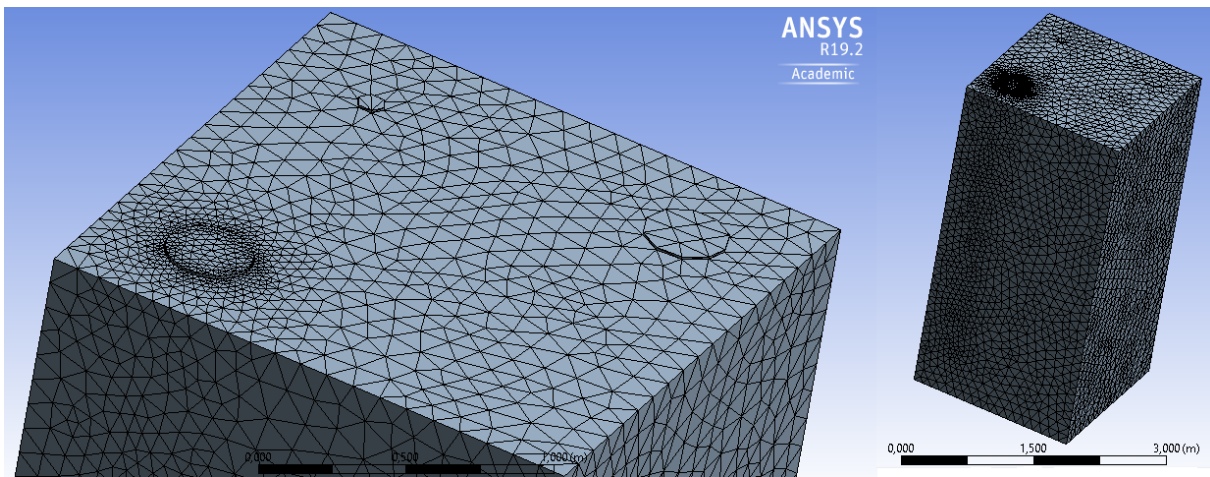


Figure 15. Improved mesh in ANSYS FLUENT.

The resulted mesh conditions for the simulation are shown in the figure 16. In this picture, it is possible to see the maximum value of skewness for some tetrahedron (0.89717) and its average (0.23225) throughout the geometry.

Details of "Mesh"	
Quality	
Check Mesh Qua...	Yes, Errors
<input type="checkbox"/> Target Skewn...	Default (0.900000)
Smoothing	Medium
Mesh Metric	Skewness
<input type="checkbox"/> Min	3,0917e-007
<input type="checkbox"/> Max	0,89713
<input type="checkbox"/> Average	0,23225
<input type="checkbox"/> Standard Devi...	0,12108
Inflation	
Advanced	
Statistics	
<input type="checkbox"/> Nodes	97596
<input type="checkbox"/> Elements	510285

Figure 16. Skewness and Statistics of the improved mesh.

In the figure 17, the mesh metric is revealed, in which less than 500 elements presented high skewness while the others have excellent and good cell quality. The total number of nodes and elements within the mesh are 97596 and 510285 respectively.

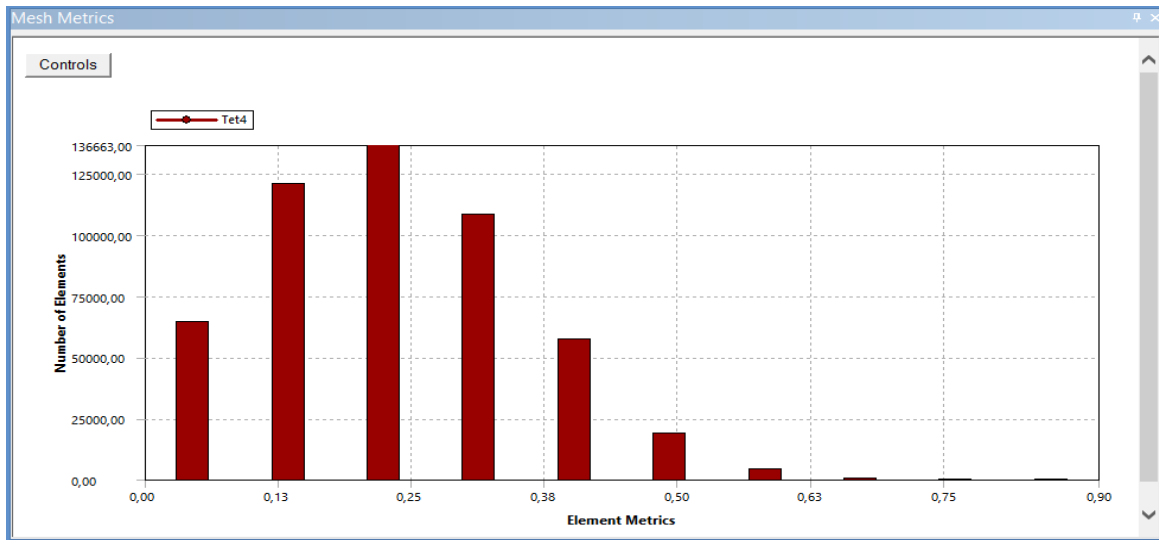


Figure 17. Mesh metric of the improved mesh.

6.2 LNG vaporization configuration within ANSYS

The figure 18 illustrates the final configuration of the LNG vaporization in ANSYS FLUENT, The key and success of the simulation convergence within this setting relies on 2 pillars, the right and suitable configuration of the mesh, and the selection of the mass transfer mechanism from the LNG phase to air phase, called the evaporation-condensation Lee model. This model was made for considering boiling condition, which is the case of this thesis (LNG vaporization phenomenon). The advantage of this configuration is that it can be used as starting point for other LNG vaporization studies with ANSYS.

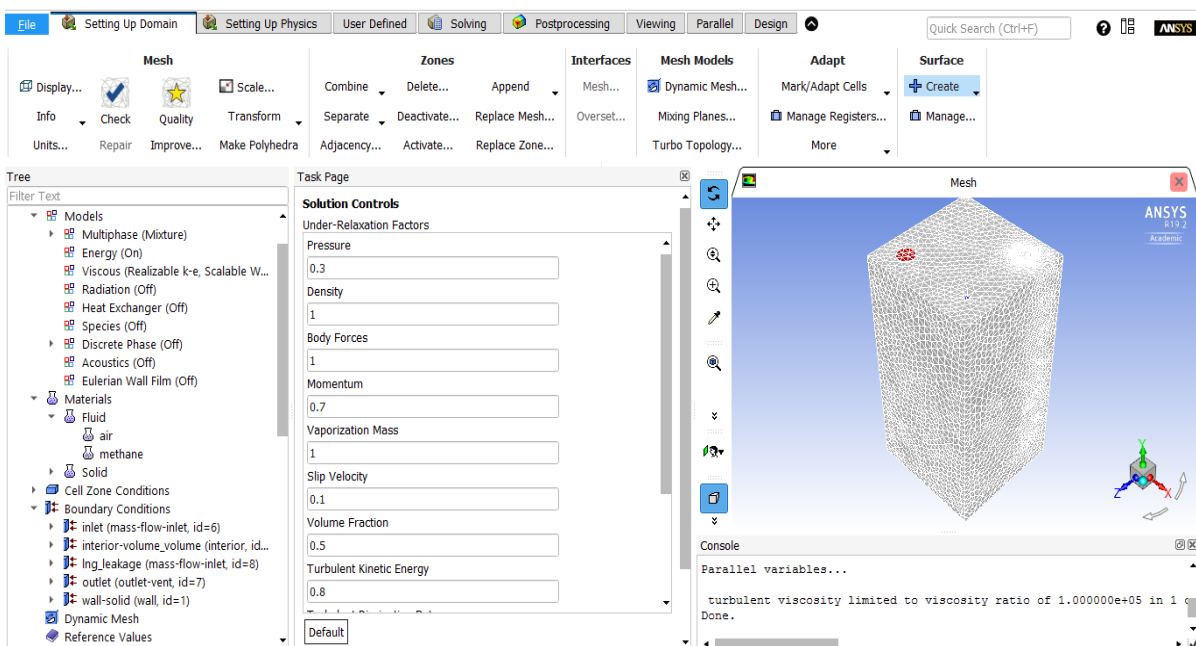


Figure 18. LNG vaporization set up in ANSYS FLUENT.

6.3 Post-processing of variables

The planned simulations were run for 5, 15, and 25 seconds, however, the 5 and 15 seconds cases were successful converged and the 25 seconds case was unstable for this configuration, therefore, a case of 20 seconds was run for replacing the latter. Numerous times of 25 seconds case were run, nevertheless, ANSYS detected divergence in all those times, reason why it had to be changed. For the case of 5 seconds case the time step, number of time step and maximum iterations were 1 (s), 5 and 5 respectively. For the case of 15 seconds case, 1 (s), 15, 15, and for the 20 seconds case 1 (s), 20, 20 accordingly.

6.3.1 LNG volume fraction

The figure 19 shows the evaporation and the LNG volume fraction inside the TCS after 5 seconds leakage and that condition remains constant with no changes after 15 and 20 second. It is clear to see that as soon as it enters the TCS the LNG is vaporized and when it reaches around 1 m in the bottom direction, the LNG fully changes phase to gas. This behavior is explained due to 2 factors: the LNG is undergoing a flash vaporization phenomenon due to the expansion and the high pressure conditions (12 Bar) increases the boiling point of LNG above 111.15 K, facilitating the phase change.

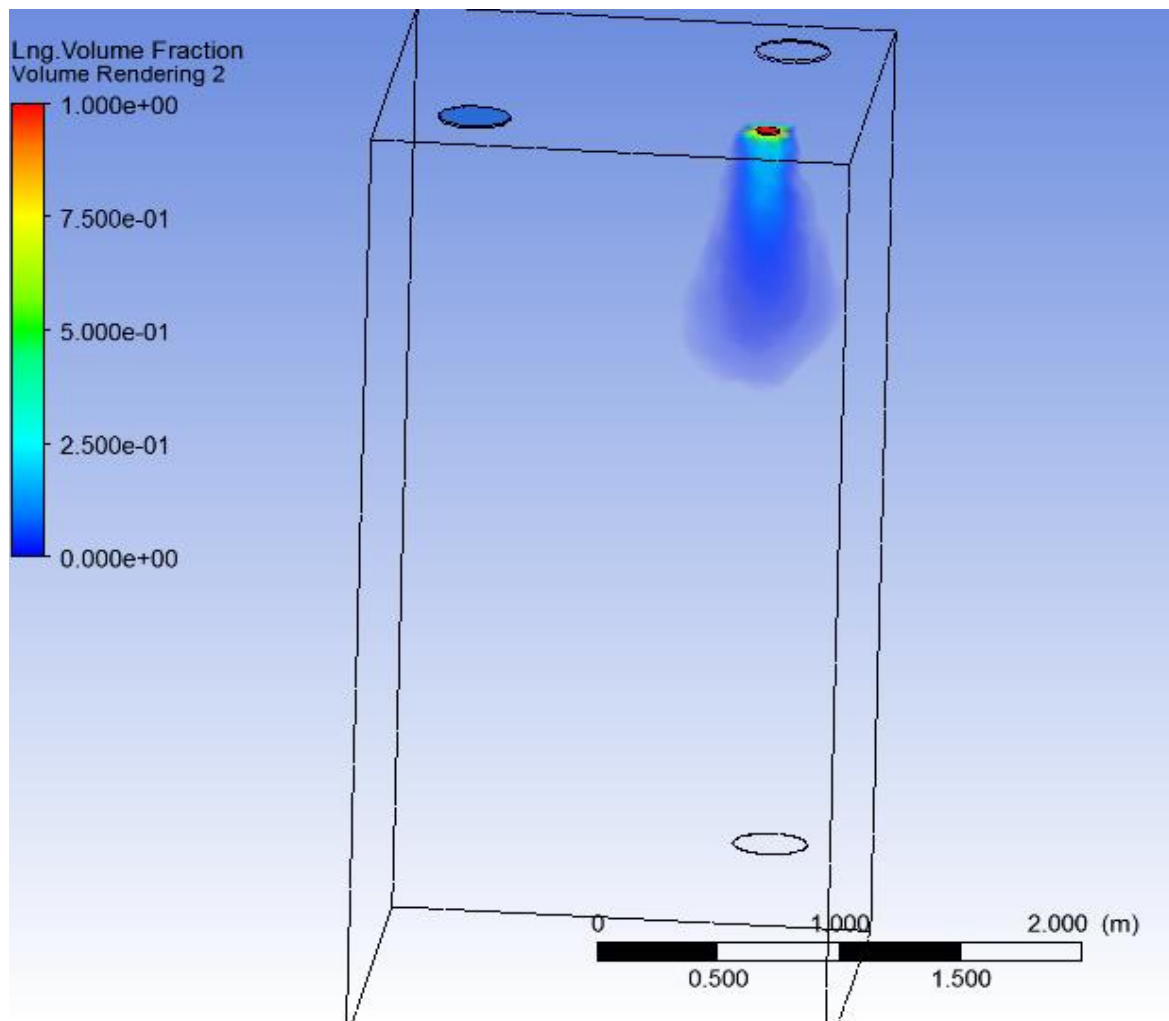


Figure 19. LNG volume fraction inside TCS.

6.3.2 Fluids flow velocity

The arrows, in the figure 20, 21, 22 reveal the fluid flow velocity after 5, 15 and 20 seconds of leakage respectively, and indicate the direction of the fluids. It is also possible to notice in the figure 21, high concentration of gas near the walls, flowing toward the vent outlet. In the figure 22, after a certain time the system is stabilized and all gas is removed in the vent outlet.

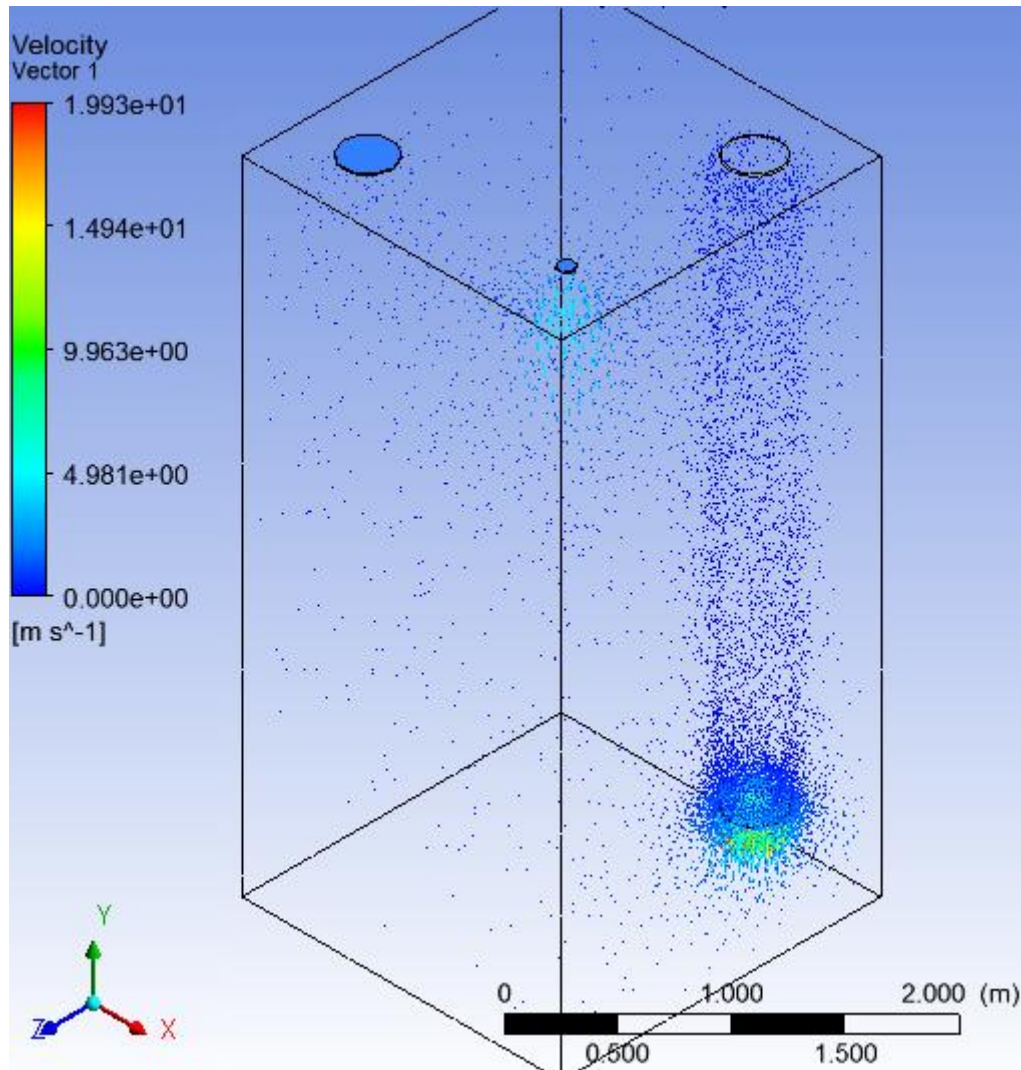


Figure 20. Fluids flow velocity after 5 s.

The figure 23 illustrates an important phenomenon after the evaporation of the LNG, while the gas is flowing. It is that a certain amount of gas enters inside the pipe (vent inlet) as indicated with blue arrows with an approximate velocity of 5 m/s. This gas behavior should be considered within the design of the vent inlet for the TCS, as it might interrupt operational conditions of the vent inlet.

In addition, the figure 24 illustrates the streamlines of the velocity of the fluids and it can be noticed the movements of the fluids going from the LNG vaporization point to the vent outlet areas (black arrow). This result was expected since the beginning, however, the fluids follow a spiral trajectory probably due to a change of velocity and density, during LNG vaporization.

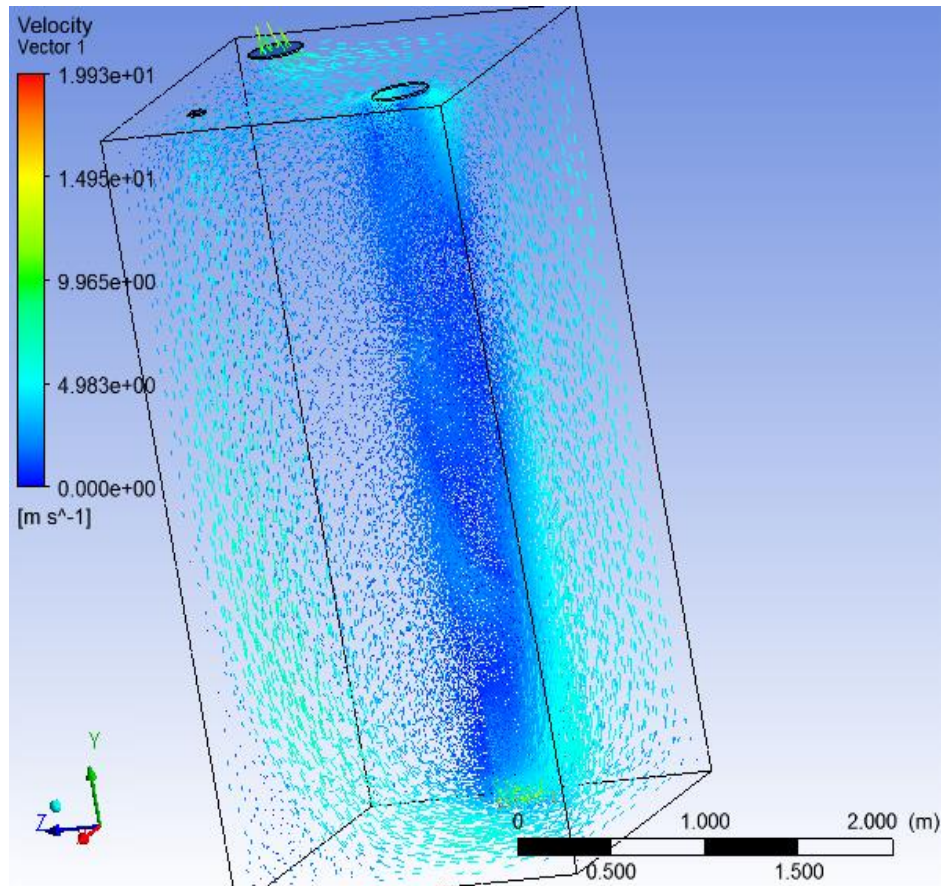


Figure 21. Streamlines of the velocity of the fluids 15 s.

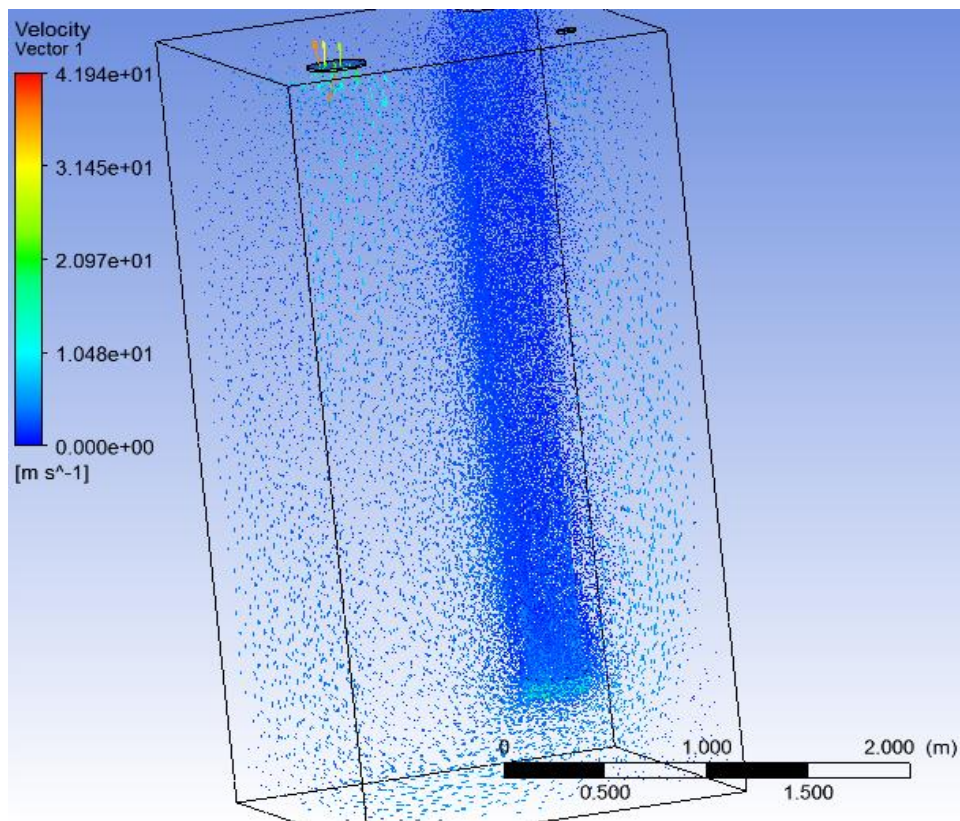


Figure 22. Fluids flow velocity after 20 s.

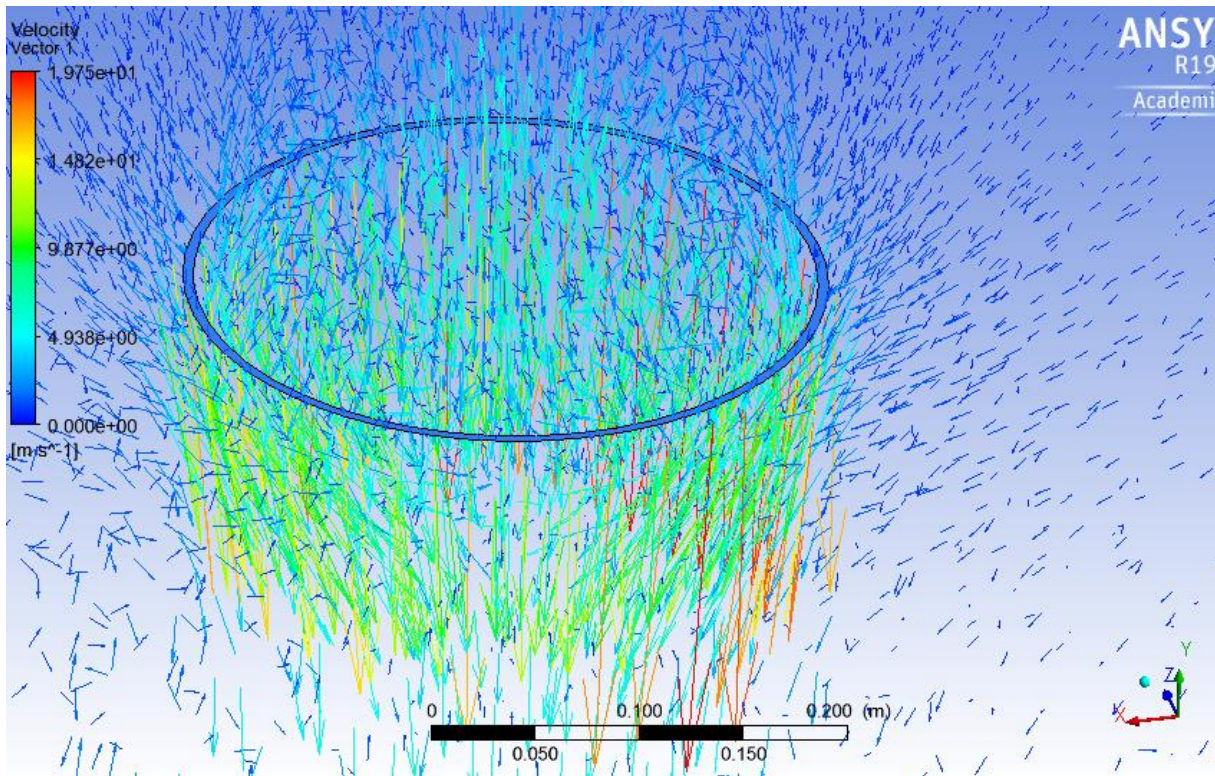


Figure 23. Velocity of the fluids.

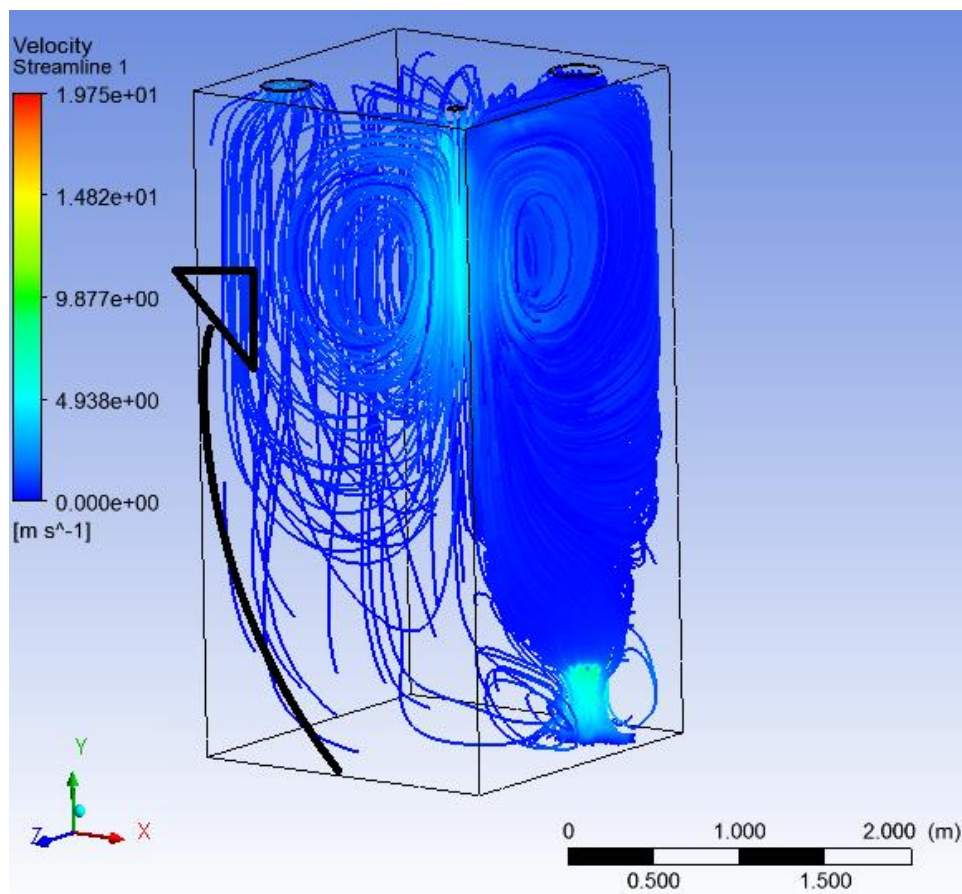


Figure 24. Streamlines of fluids velocity.

6.3.3 Gradient pressure results

The figure 25 reveals the gradient pressure contours throughout the TCS from up to the bottom. It is possible to see that pressure increases in the same way that the LNG is being evaporated, reaching a maximum increase of around 30 Pa in the bottom. This case is applicable for the 3 studied cases in which after 5 seconds leakage, the behavior of the leakage is the same.

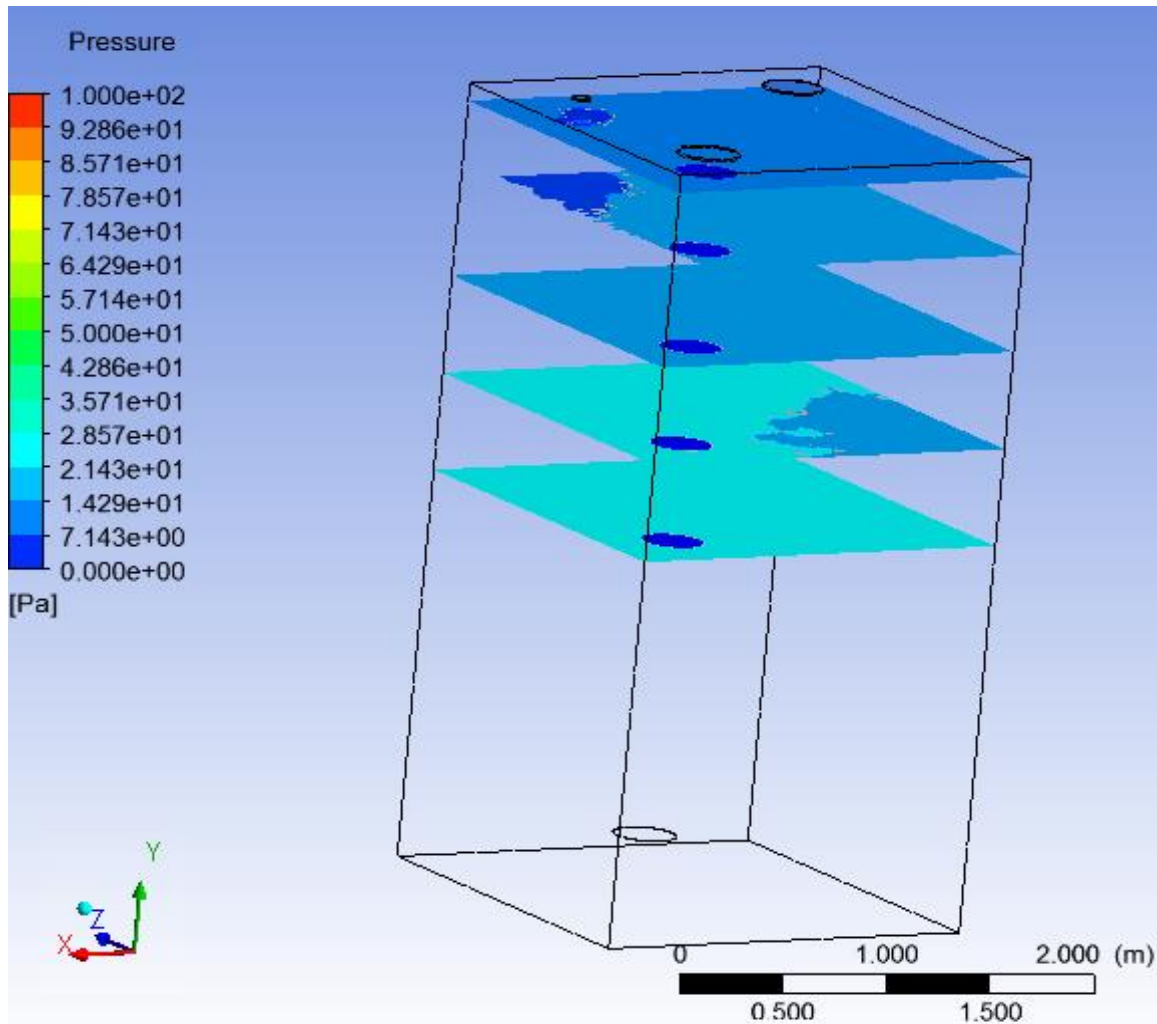


Figure 25. Gradient pressure contours.

6.3.4 Temperature results

For the temperature, the obtained results are the same for the 3 cases (5, 15 and 20 seconds). The figure 26 shows the temperature of the TCS with a slight change in the vicinity of the LNG leakage. It means that when the LNG is being evaporated, the surroundings become cold. Further down, the temperature tends to increase until reaching normal temperature (288 K) as the ventilation system is removing the gas to the vent outlet, avoiding the gas get in contact with materials.

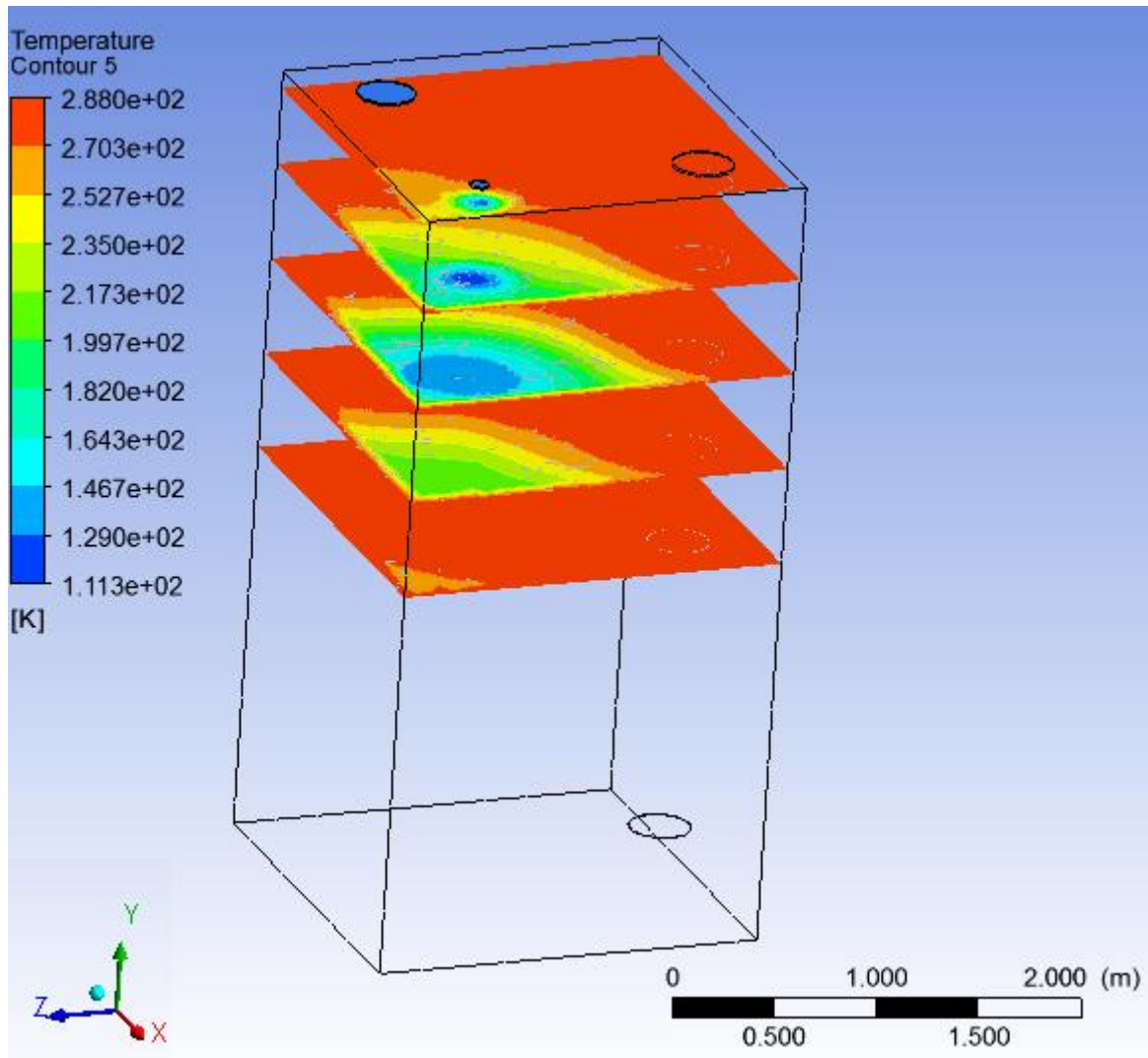


Figure 26. Temperature contours.

7 RECOMMENDATIONS

The original TCS model was simplified and introduced into the simulation, with the ultimate goal of understanding the vaporization phenomenon and its implications, more easily. Therefore, some unrealistic results were obtained after simulating the proposed case. For improving those results, the first step to be taken is to refine the mesh. In this thesis, as a student license was used for ANSYS, there is one critical limitation for the maximum number of cells or elements that can be used, for discretizing the geometry, up to 512000 cells. It automatically increases the error in the obtained results. Thus, the implementation of a professional license allows having high quality and more discretized mesh. Similarly, using a powerful machine that can handle a greater number of iterations might optimize time consumption during simulations, consequently, smooth and friendly results in terms of visualization the color spectrum that ANSYS uses for displaying results.

The studied case was configured as simple as possible for doing the simulation smooth, therefore, when the escalation to the real LNG marine system takes place, it is highly important to start from the simplified model to the real geometry by doing small changes, facilitating convergence, taking in account that the complexity of ANSYS might lead to divergences.

On the other hand, a possible source of error in this thesis was the absence of the ventilation pressure difference that might induce the air inlet, dragging the vaporized gas to the vent outlet. Therefore, it can be included in future simulations, starting with 10-20 mbar in vent inlet. Some experts suggest that it might be run without LNG leakage (just flowing air inside TCS), in order to calculate and check air flow conditions, and then leakage can be included in the model.

8 CONCLUSIONS

Based on the LNG volume fraction results, the concentration of gas is dispersed along the TCS, except by certain areas near to the leakage hole (1 meter down from the hole), in which some concentration of LNG can be found. According to the presented results, the LNG leakage immediately starts to be vaporized when entering the TCS without forming any jet. The resulted increase in the pressure is around 0.3 mbar which is not a considerable increment that might damage the infrastructure inside the TCS in the case of leakage. However, based on other calculations made by HeLeNGi indicate that this pressure gradient might increase up to 170 mbar. Therefore, as this type of studies has not been done before in the world, it is difficult to obtain a decisive conclusion of this case, reason why the results must be compared to real experimental data in which at the same time are expensive and costly, even though, they have to be performed.

The configuration and set up of the LNG vaporization system on ASNYS was performed, therefore, it might be a starting point for continuing with the project for improving the actual conditions of this case. For example, refining the mesh and reducing the time step size of the simulation and increasing the number of iterations, to have more accurate results after iterations.

The ventilation system of 30 times the TCS volume per hour is vital for having a safe design of the LNG marine system, as this value guaranty a recirculation of the formed gas (toward the vent outlet) in the case of leakage. The fact of removing, as fast as possible, any vaporized gas brings 2 advantages, cutting down the risk of explosion due to high pressure and reducing the exposure time of the cold gas with pipes and valves, avoiding any possible damages in materials caused by thermal shock.

REFERENCES

Afs.enea.it. (2019). *ANSYS FLUENT 12.0 Theory Guide - 18.3.1 Spatial Discretization*. Retrieved from: <http://www.afs.enea.it/project/neptunius/docs/fluent/html/th/node366.htm>

Ansyshelp.ansys.com. (2019). - *ANSYS Help*. Retrieved from: https://ansyshelp.ansys.com/account/secured?returnurl=/Views/Secured/corp/v192/flu_ug/flu_ug_reference_values_task_page.html

ANSYS, Inc (2018). *ANSYS Fluent Tutorial Guide*. 18. Canonsburg, PA SAS IP, Inc, pp.1-1034. Retrieved from: <http://users.abo.fi/rzevenho/ansys%20fluent%2018%20tutorial%20guide.pdf>

ANSYS,Inc (2006). *ANSYS CFX-Solver Theory Guide*. 11. Canonsburg, PA: ANSYS Europe, Ltd, pp.1-297. Retrieved from: <http://product.caenet.cn/Uploadfiles/12872437250986625020081129090050986.pdf>

ANSYS, Inc (2013). *ANSYS Fluent Theory Guide*. 15. Canonsburg, PA: SAS IP, Inc, pp.1-759. Retrieved from: <http://www.pmt.usp.br/ACADEMIC/martoran/NotasModelosGrad/ANSYS%20Fluent%20Theory%20Guide%2015.pdf>

BUREAU VERITAS (2017). *Gas Filled Ships- International Code of Safety for Ships Using Gases or other Low-Flashpoint Fuels (IGF Code*. NR 529. Paris: Bureau Veritas Marine & Offshore.

China Classification Society (2013). *Rules for natural gas filled ships*. Retrieved from: <http://www.ccs.org.cn/ccswzen/font/fontAction!moudleIndex.do?moudleId=84>

Courses.edx.org. (2018). *A Hands-on Introduction to Engineering Simulations*. Retrieved from: Available at: <https://courses.edx.org/courses/course-CornellX+ENGR2000X+1T2018/course/> [Accessed 7 Dec. 2019].

DNV GL (2014). *LNG as Fuel Ship*. Hamburg: DNV GL Maritime Communication, pp.1-28. Retrieved from: https://www.dnvgl.com/Images/LNG_report_2015-01_web_tcm8-13833.pdf

European Union (2015). *LNG Fueled Vessels Design Training*. Glasgow: University of Strathclyde, pp.1-150. Retrieved from: <https://www.onthemosway.eu/wp-content/uploads/2015/06/Lecture-Notes.pdf>

Health and Safety Laboratory (2010). *LNG source term models for hazard analysis*. RR789. Buxton: Crown, pp.1-70. Retrieved from: <http://www.hse.gov.uk/research/rrpdf/rr789.pdf>

International Gas Union (2015). *Small Scale LNG*. Paris: World Gas Conference, pp.1-84. Retrieved from: http://www.igu.org/sites/default/files/node-page-field_file/SmallScaleLNG.pdf

International Gas Union (2017). *Enabling Clean Marine Transport*. Barcelona: International Gas Union (IGU), pp.1-30. Retrieved from: https://www.igu.org/sites/default/files/node-document-field_file/IGU_A4_CleanMarineTransport_Final%20March%202017_4.pdf

Karlsson, S., Högnabba, T., & Kuusisaari, M. (2013, May 17). The wartsila gas valve unit enclosed design (gvu-ed) for marine applications. *Wärtsilä Technical Journal*, 1-4. Retrieved from: <https://www.wartsila.com/twentyfour7/in-detail/the-wartsila-gas-valve-unit-enclosed-design-gvu-ed-for-marine-applications>

Kim, K., Kang, H., Choung, C. and Park, J. (2011). On the Application of CFD Codes for Natural Gas Dispersion and Explosion in Gas Fuelled Ship. *Journal of the Korean Society of Marine Engineering*, 35(7), pp.946-956. Retrieved from: <https://www.sciencedirect.com/science/article/pii/S0304389406012301>

Le Fevre, C. (2018). A review of demand prospects for LNG as a marine transport fuel. *THE OXFORD INSTITUTE FOR ENERGY STUDIES*, NG 133. Retrieved from: <https://www.oxfordenergy.org/publications/review-demand-prospects-lng-marine-fuel/>

Li, L., Choi, J., Bang, J., Lee, S., Lee, S. and Kim, D. (2017). Numerical investigation of LNG gas dispersion in a confined space: An engineering model. *Journal of Mechanical Science and Technology*, 31(9), pp.4533-4540. Retrieved from: <https://link.springer.com/article/10.1007/s12206-017-0853-2>

Li, X., Zhou, R. and Konovessis, D. (2016). CFD analysis of natural gas dispersion in engine room space based on multi-factor coupling. *Ocean Engineering*, 111, pp.524-532. Retrieved from: <https://www.sciencedirect.com/science/article/pii/S0029801815006319>

Löhner, R. (2001). *Applied CFD techniques*. 1st ed. New York: Wiley.

Marine Service Noord (2019). *LNG Fuel System for Inland and Short Sea Shipping*. Hoogezand, pp.1-4.

Mokhatab, S. (2014). Natural Gas Liquefaction. In: S. Mokhatab, J. Mak, J. Valappil and D. Wood, ed., *Handbook of Liquefied Natural Gas*, 1st ed. Oxford: Gulf Professional, pp.147-183. Retrieved from: ProQuest Ebook Central, <https://ebookcentral.proquest.com/lib/uisbib/detail.action?docID=1511054>.

Nguyen, K. (2015). Design Optimization of a Low Pressure LNG Fuel Supply System. M.Sc. Norwegian University of Science and Technology. Retrieved from <https://ntnuopen.ntnu.no/ntnu-xmlui/handle/11250/2374408>


Nilsen, O. (2018). *LNG regulatory update “Best fuel of the future”*. Retrieved from: <http://www.golng.eu/files/Main/20180417/2.%20Ole%20Vidar%20Nilsen%20-%20DNV%20GL.pdf>

Sung, K., Bang, J., Li, L., Choi, J., Kim, D., Ryou, H., Yoon, K. and Lee, S. (2016). Effect of crack size on gas leakage characteristics in a confined space. *Journal of Mechanical Science and Technology*, 30(7), pp.3411-3419. Retrieved from: <https://link.springer.com/article/10.1007/s12206-016-0650-3>

Wendt, J. (2009). *Computational Fluid Dynamics*. 12th ed. Berlin, Heidelberg: Springer Berlin Heidelberg, pp.15-51. Retrieved from: <https://www.springer.com/gp/book/9783540850557>

Appendices

Appendix 1 – ANSYS REPORT

<p>Contents</p> <p>1. File Report Table 1 File Information for TCS3</p> <p>2. Mesh Report Table 2 Mesh Information for TCS3 Table 3 Mesh Statistics for TCS3</p> <p>3. Physics Report Table 4 Domain Physics for TCS3 Table 5 Boundary Physics for TCS3</p> <p>4. Pictures</p>	 <p>Title Generic Report</p> <p>Date 2019/06/13 18:37:05</p>
--	---

1. File Report

Table 1. File Information for TCS3

Case	TCS3
File Path	C:\Users\danny\Desktop\UiS\4th semester (Thesis)\1) STATE OF THE ART\CFDTool\Helengi\TCS naviin\Desde cero VOF -extrude geometry 4\intento 8 con naviin air inlet abajo MIX el mejor_files\dp0\FFF\Fluent\FFF.1-36-00020.dat.gz
File Date	08 junio 2019
File Time	09:05:13 p. m.
File Type	FLUENT
File Version	19.2.0

2. Mesh Report

Table 2. Mesh Information for TCS3

Domain	Nodes	Elements	Tetrahedra	Wedges	Pyramids	Hexahedra	Polyhedra
solid	97656	510766	510766	0	0	0	0

Table 3. Mesh Statistics for TCS3

Domain	Minimum Face Angle	Maximum Face Angle	Maximum Edge Length Ratio	Maximum Element Volume Ratio	Connectivity Range
solid	4.75197 [degree]	130.764 [degree]	12.0713	49.0217	1 40

3. Physics Report

Table 4. Domain Physics for TCS3

Domain - solid	
Type	cell

Table 5. Boundary Physics for TCS3

Domain	Boundaries
solid	Boundary - inlet
	Type MASS-FLOW-INLET
	Boundary - Ing_leakage
	Type MASS-FLOW-INLET
	Boundary - outlet
	Type PRESSURE-OUTLET
Boundary - wall solid	
Type WALL	